Magnetically Driven Implosions for Inertial Confinement Fusion at Sandia National Laboratories

M. E. Cuneo, *Senior Member, IEEE*, M. C. Herrmann, D. B. Sinars, S. A. Slutz, W. A. Stygar, R. A. Vesey, A. B. Sefkow, G. A. Rochau, G. A. Chandler, J. E. Bailey, J. L. Porter, R. D. McBride, D. C. Rovang, M. G. Mazarakis, E. P. Yu, D. C. Lamppa, K. J. Peterson, C. Nakhleh, S. B. Hansen, A. J. Lopez, M. E. Savage, C. A. Jennings, M. R. Martin, R. W. Lemke, B. W. Atherton, I. C. Smith, P. K. Rambo, M. Jones, M. R. Lopez, P. J. Christenson, M. A. Sweeney, B. Jones, L. A. McPherson, E. Harding, M. R. Gomez, P. F. Knapp, T. J. Awe, R. J. Leeper, C. L. Ruiz, G. W. Cooper, K. D. Hahn, J. McKenney, A. C. Owen, G. R. McKee, G. T. Leifeste, D. J. Ampleford, E. M. Waisman, A. Harvey-Thompson, R. J. Kaye, M. H. Hess, S. E. Rosenthal, and M. K. Matzen

(Invited Paper)

***Abstract*—High current pulsed-power generators efficiently store and deliver magnetic energy to z-pinch targets. We review applications of magnetically driven implosions (MDIs) to inertial confinement fusion. Previous research on MDIs of wire-array z-pinches for radiation-driven indirect-drive target designs is summarized. Indirect-drive designs are compared with new targets that are imploded by direct application of magnetic pressure produced by the pulsed-power current pulse. We describe target design elements such as larger absorbed energy, magnetized and pre-heated fuel, and cryogenic fuel layers that may relax fusion requirements. These elements are embodied in the magnetized liner inertial fusion (MagLIF) concept [Slutz *et al.* "Pulsed-power-driven cylindrical liner implosions of laser pre-heated fuel magnetized with an axial field," Phys. Plasmas, 17, 056303 (2010), and Stephen A. Slutz and Roger A. Vesey, "High-Gain Magnetized Inertial Fusion," Phys. Rev. Lett., 108, 025003 (2012)]. MagLIF is in the class of magneto-inertial fusion targets. In MagLIF, the large drive currents produce an azimuthal magnetic field that compresses cylindrical liners containing pre-heated and axially pre-magnetized fusion fuel. Scientific breakeven may be achievable on the Z facility with this concept. Simulations of MagLIF with deuterium-tritium fuel indicate that the fusion energy yield can exceed the energy invested in heating the fuel at a peak drive current of about 27 MA. Scientific breakeven does not require alpha particle self-heating and is therefore not equivalent to ignition. Capabilities to perform these experiments will be developed on Z starting in 2013. These simulations and predictions must be validated against a series of experiments over the next five years. Near-term experiments are planned at drive currents of 16 MA with D_2 fuel. MagLIF increases the efficiency of coupling energy (=target absorbed energy/driver stored energy) to targets by 10–150X relative to indirect-drive targets. MagLIF also increases the absolute energy absorbed by the target by 10-50X relative to indirect-drive targets. These increases could lead to higher fusion gains and yields. Single-shot high yields are of great utility to national security missions. Higher efficiency and higher gains may also translate into more compelling (lower cost and complexity) fusion reactor designs. We will discuss the broad goals of the emerging research on the MagLIF concept and identify some of the challenges. We will also summarize advances in pulsed-power technology and pulsed-power driver architectures that double the efficiency of the driver.**

***Index Terms*—Direct-drive, fusion targets, indirect-drive, inertial confinement fusion (ICF), liners, magnetized liner inertial fusion (MagLIF), magnetized target fusion, magneto-inertial fusion (MIF), pulsed power, z-pinches.**

I. Introduction

HIGH current pulsed-power generators efficiently store and deliver magnetic energy to a variety of high energy density physics experiments. The Z pulsed-power facility at Sandia National Laboratories is a low-inductance pulsed-power driver that delivers a peak current of 10 to 26 MA, with adjustable current pulse shapes of durations from 100 to 1000 ns. The magnetic drive pressure provided by this technology is extraordinarily diverse in application [1]. Z provides a rich opportunity to study the science and applications of cylindrical magnetically driven implosions (MDIs). Cylindrical MDI of wire-array z-pinches have produced nearly blackbody soft X-ray sources [2], and the most intense laboratory sources of multi-keV X-ray line radiation [3], [4]. Dynamic material properties such as the equation of state or strength of a material are measured with unprecedented accuracy with planar magnetically-driven platforms that produce shocked-compressed or isentropically compressed states of matter [5], [6]. More than half of the experiments on Z today are performed on dynamic materials platforms that did not exist a little more than 10 years ago [7]–[11].

MDIs of wire array z-pinches were extensively studied on the Z facility over the period of 1997–2006. More than 140 publications resulted on wire array implosion and stagnation physics, on the scaling and optimization of wire array output, and on the uses of such X-ray sources. A recent extensive review of the dense z-pinch summarizes the previous and

Manuscript received May 1, 2012; revised September 17, 2012; accepted October 2, 2012. Date of publication November 15, 2012; date of current version December 7, 2012. Sandia National Laboratories is a multi-program laboratory managed and operated by Sandia Corporation, a wholly owned subsidiary of Lockheed Martin Corporation, for the U.S. DOE's NNSA under contract DE-AC04-94AL85000.

The authors are with Sandia National Laboratories, Albuquerque, NM 87185-1193 USA (e-mail: mecuneo@sandia.gov).

Digital Object Identifier 10.1109/TPS.2012.2223488

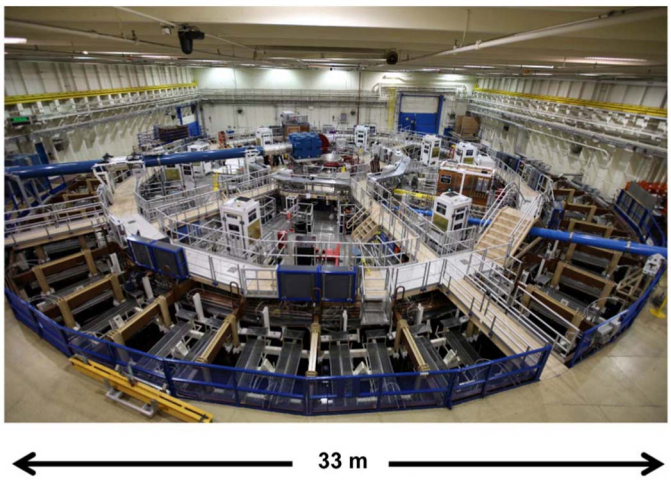

Fig. 1. The Z facility and high bay, after the refurbishment was completed in 2007.

current status of wire array physics [12]. At that time, wire array z-pinches on the Z facility produced the highest soft X-ray power and total X-ray energy of any laboratory facility in existence. Total soft X-ray energies of 1.8 MJ were produced at an efficiency of 15%, relative to the total stored energy (11.4 MJ) [13]. These X-ray sources are utilized for National Nuclear Security Agency (NNSA) national security missions, for laboratory astrophysics, as well as for indirect-drive inertial confinement fusion (ICF). Two indirect-drive ICF concepts based on wire array z-pinch radiation sources were explored in parallel: the "z-pinch-dynamic-hohlraum" (ZPDH) [14]–[22], and the "double-ended hohlraum" (DEH) [23]–[27]. The DEH is also referred to as the double-z-pinch-driven hohlraum. X-ray energies of order 200 kJ (ZPDH) to 700 kJ (DEH) were coupled to hohlraums in order to drive ICF capsules on Z. Significant progress was made on both concepts prior to the Z refurbishment project, summarized in Section III.

Our research program is centered on experiments on the Z pulsed-power generator [28], [29]. Z is a compact, MJ-class fusion target physics platform. The facility is of order 1000 m^2 and stores up to 21 MJ at 85 kV charging voltage. Fig. 1 is a photograph of the Z facility, showing the top of the 33-m diameter circular tank. The facility was entirely refurbished in 13 months for about 4$/Joule. The refurbishment doubled the stored energy and increased the peak currents possible from 20 to 26 MA into low impedance loads.

The overarching goal of the pulsed-power fusion research program is to establish the science and technology of MDIs for stockpile stewardship applications. By advancing our understanding of what is possible with pulsed power, we are developing innovative platforms that are applied to many important stewardship questions. For fusion science, we will assess the fusion conditions that can be created with MDIs, assess how those conditions can be scaled to larger yields of interest on existing and future facilities, develop predictive simulations, and maximize the fusion target gains and yields with the smallest possible pulsed-power driver. In particular, we will evaluate the feasibility of reducing laboratory fusion ignition requirements with MDI targets. Pulsed-power fusion target designs have different failure modes than other concepts and therefore serve as risk mitigation for ignition in the laboratory today, and high fusion yields in the future. Large single-shot fusion yields are of long-term interest for the stockpile stewardship program.

Pulsed-power fusion research on Z is now exploring approaches that use magnetic pressure to directly compress solid liners containing fusion fuel. Direct drive eliminates several intermediate steps in the process of coupling the energy stored by the generator into the kinetic energy of imploding fuel, making it potentially much more efficient. For example, it eliminates inefficiencies in: converting magnetic energy into soft X-rays, coupling the soft X-rays to a hohlraum, the hohlraum re-emission (wall albedo), coupling from primary to any secondary hohlraums, and the conversion of X-ray drive on a capsule target into fuel kinetic energy through capsule ablation and the rocket effect. Peak currents of 26 MA can generate direct-drive magnetic pressures of 100 MBar and couple 500 kJ to cm-scale targets, far in excess of what can be obtained with any pulsed-power indirect-drive target designs on Z. Direct drive is as much as $20X$ (ZPDH) to $150X$ (DEH) times more efficient at coupling driver energy to the fusion fuel. Increased coupling efficiency comes with increased risk of instabilities that can prevent fusion and potentially, unknown risks. The study of instabilities of MDIs is an important aspect of our research program.

MDI concepts that combine up to six critical target design characteristics or elements may relax the requirements to achieve significant fusion conditions:

(i) cylindrical liner target geometry,
(ii) direct drive using magnetic pressure to deliver increased energy to large targets with large volumes of fuel,
(iii) axially pre-magnetized deuterium $(\mathrm{D_2})$ or deuterium-tritium (DT) gaseous fuel,
(iv) magnetic flux compression to magnetize the fuel,
(v) pre-heating of the fuel before or during the implosion, and
(vi) the possibility of cryogenic fuel layers.

These elements are embodied in the magnetized liner inertial fusion or "MagLIF" [30], [31] concept and are discussed more completely in Section IV. Integrated MagLIF target designs predict that DT fusion yields of order 100 kJ may be possible on Z at peak drive currents of about 27 MA, reaching fuel pressures of a few GBar. This yield would represent *scientific breakeven* where the fusion energy output $(\mathrm{E_{fusion}})$ equals the energy invested in heating the fuel $(\mathrm{E_{fuel}})$. This is sometimes represented by the condition $\mathrm{Q_{HS}} = 1$, where $\mathrm{Q_{HS}} = \mathrm{E_{fusion}}/\mathrm{E_{fuel}}$ is the gain of the hot spot. Scientific breakeven, to our knowledge, has never been achieved in any laboratory fusion system to date. Scientific breakeven is not ignition because alpha particle heating is not required. Such yields were never achieved in any target designs for indirect-drive concepts on Z, either before or after the refurbishment.

The goal of this paper is to document the change in direction of the pulsed-power fusion program in the context of past work. We will discuss the broad goals of the emerging research on the MagLIF concept and identify some of the challenges in integrating the new target design elements. A number of papers have been published or submitted on the detailed MagLIF

target designs [30], [31], on dedicated instability and implosion experiments [32]–[37], and on related systems [38]–[40]. These MagLIF simulations and MDI target design elements must be validated against experiments. An extensive campaign of integrated experiments will be carried out over the next five years, discussed below.

Section II discusses the requirements for hot-spot ignition, and target design elements that may reduce fusion requirements. Section III summarizes progress on MDIs for indirect-drive pulsed-power concepts in the period 1997–2006. Section IV describes the potential of MDIs for direct magnetic drive of fusion targets, and MagLIF in the context of other direct-drive concepts that have been proposed. Section V compares indirect and direct-drive target design performance. These designs were based on radiation hydrodynamic (2D-RHD) and radiation Magneto-hydrodyamic (2D-RMHD) simulations for 100-ns class pulsed-power generators. Section VI briefly summarizes advances in pulsed-power technology that doubles the efficiency of the pulsed-power driver. Section VII concludes the discussion. Possible application of this work to inertial fusion energy (IFE) is discussed very briefly in Section VII.

II. Challenge of Ignition and Gain and Advantages of Direct Drive and Fuel Magnetization

Three conditions are required to achieve significant fusion yields [41]–[44]. First, the fuel temperature must be raised above the ideal ignition temperature of 4.3 keV for an equimolar mixture of DT in order to overcome Bremsstrahlung radiation losses that cool the plasma. In laser-driven ICF, the fuel is self-heated with rapid spherical target implosion velocities ($\sim$30$-$40 cm/μs). Second, alpha particle energy must be deposited in the hot spot to permit fusion particle heating to temperatures closer to the peak of the fusion reaction rate. This requires the assembled fuel hot spot $\rho R_{HS} \sim 0.2-0.6$ g/cm^2, greater than the range of the alpha particles. Control of instabilities during implosion of the target is required to prevent the hot spot from cooling due to mixing with the colder target. Finally, high ρR in the fuel and remaining ablator mass is required for efficient fuel burn up before the capsule disassembles. Requirements on the assembled fuel of $\rho R \sim 3$ g/cm^2 allow 30% of the fuel to be burned up before disassembly. Formation of a cold and dense fuel layer surrounding the hot spot requires highly symmetric assembly of the target.

The requirements for hot spot ICF ignition and gain are extremely challenging. The conditions in the hot spot are equivalent to $\sim 10^{12}$ Bars (1 TBar) [44]. This state must be achieved in a controlled manner with the hot spot surrounded by a symmetric distribution of cold fuel, and with minimum interface area. The difficulty of producing such a stagnated plasma state underscores the immense challenges of conventional hot spot ignition. Achieving this configuration through spherical convergence of imploding capsules requires exquisite control over many factors, including drive pulse shape and shock timing, radiation drive symmetry, control of instability growth, coupling of radiation to the target, unprecedented precision in target fabrication and metrology, and many others. Highly integrated experiments are currently underway on the National Ignition Facility (NIF) to demonstrate ignition and gain in the laboratory with indirect drive [45].

Hot spot ignition conditions of $\rho R_{HS} \sim 0.6$ g/cm^2 and hot spot temperatures $T_{HS} \sim 5$ keV are equivalent to a requirement on the so-called "triple product":

$$(\rho RT)_{HS} \approx 3 \left[\frac{g - \text{keV}}{\text{cm}^2}\right]. \tag{1}$$

Treating the DT hot spot with an ideal gas equation of state [44], we find

$$P[Bar] = 7.7e8\rho \left[\frac{g}{\text{cm}^3}\right] T_i[\text{keV}]. \tag{2}$$

Substituting the triple product condition (1) into the equation of state (2) yields:

$$PR \sim 2.3e9\,[Bar - \text{cm}] = 23[TBar - \mu\text{m}]. \tag{3}$$

The total energy content of the hot spot plasma is estimated as

$$E \sim \frac{3}{2}PV \sim \frac{3}{2}P\left(\frac{4\pi}{3}R^3\right) \sim 1.4e9R^2[\text{cm}^2](J) \sim 14R^2[\mu\text{m}^2][J]. \tag{4}$$

The numerical value is obtained by substituting from (3) for the pressure-radius product, PR. The hot spot for capsules on the NIF will absorb about 15 kJ of kinetic energy during implosion [41], which is about 10% of the total energy absorbed by the capsule. Solving (4) yields $E_{NIF} \sim 15kJ \Rightarrow R \sim 30$ μm. Substituting this radius into (3) yields a pressure $P \sim 700$ GBar. This is consistent to first order with capsule simulations [43] without burn that reach pressures of 500 GBar in the hot spot. This pressure, in (2), results in a fuel density $\rho \sim 180$ g/cm^3. Such densities require high target convergence ratios, starting from cryogenic DT fuel ($\rho \sim 0.25$ g/cm^3).

We can estimate the stagnation power required to achieve these conditions. The hot spot disassembles on an inertial time scale, roughly [42], [44]:

$$\tau_{conf} \sim \frac{R}{3c_s} = 1.2\frac{R[\mu\text{m}]}{T^{0.5}[\text{keV}]}[ps] \sim 20ps \tag{5}$$

for R $= 30$ μm and T $= 5$ keV, and for an equimolar mixture of DT. This confinement time is a lower bound because it does not account for tamping of the hot spot expansion by the surrounding cold fuel layer. An upper bound on the heating power that needs to be delivered to the hot spot is therefore:

$$P_{heat} \sim \frac{E}{\tau_{conf}} \sim 750TW. \tag{6}$$

A primary theme of this paper is to suggest that the target design elements incorporated in MagLIF may ease these requirements ($P_{heat} \sim 500$ TW, $P \sim 500$ Gbars) significantly. Simulations indicate that scientific breakeven is possible with a fuel pressure of 3 GBars.

Direct drive, either with lasers, ions, or magnetic fields, permits more energy to be absorbed by the target and coupled

to the fuel than for indirect drive, due to the elimination of inefficiencies in the intermediate conversion steps. The larger the energy delivered to the hot spot, the larger its radius can be (4). Larger delivered energy is expected to relax the requirements on achieving fusion in the laboratory. The larger the radius, the lower the hot spot pressure (3), reducing requirements on capsule drive. The lower the pressure, the lower the required ρ (2), possibly reducing requirements on fuel assembly and convergence. This is a well-known aspect of fusion target design, typically applied to scale targets to the yields required for IFE. As an example, if the energy delivered to the hot spot could be increased by a factor of $64X$ to 1 MJ, as may be possible with pulsed-power targets driven with 70 MA in 120 ns, (see Section VI), the hot spot radius could be increased a factor of $8X$ to $\sim$260 μm. This reduces the required fuel pressure by $8X$ to 90 GBars and reduces the requirement on hot spot ρ by $8X$ to 22 g/cm^3. Nuckolls recently highlighted the need to achieve higher system gains for IFE systems, and suggests that magnetic fields should be explored as an alternative method for achieving higher absorbed energy and gain [46].

Axial magnetic fields can potentially also be used to reduce the required hot spot ρR needed for self-heating provided that strong enough fields can be generated [47], [48]. The field dramatically reduces the electron thermal conduction heat loss from the plasma and effectively decreases the radial path length of alpha particles in the dense plasma by adding a Larmor rotation to the moving particle. As the ratio of the magnetic field to the fuel density B/ρ approaches infinity, the ρR required for ignition approaches zero [48]. Reduction of the ρR reduces the fuel compression requirements. For example, a reduction of the ρR from 0.3 to 0.01 g/cm^2 would reduce the required pressure by a factor of $30X$, from (3).

III. Indirect-Drive Pulsed-Power Fusion Target Designs

The Sandia pulsed-power fusion research program from 1997–2006 was primarily an assessment of the ability of MDIs of wire-array z-pinch X-ray sources to meet the many requirements for indirect-drive capsule ignition. Two indirect-drive concepts were developed to implode fusion capsules on Z [1]. The DEH was adapted from similar laser or heavy ion beam-driven hohlraum geometries by Hammer *et al.* [23]. The z-pinch dynamic hohlraum (ZPDH) was developed simultaneously in both the USSR [14] and the US [15] in the late 1970s but languished until large number wire arrays and the Z high current driver were developed as a z-pinch source [49], [50]. Fig. 2 compares scaled drawings of the two concepts as they were implemented on Z. The capsule requirements for these concepts were derived from a number of seminal works [41]–[44].

The two concepts can be thought of as extremes on a spectrum that traded maximum coupling efficiency and radiation drive temperature (ZPDH) against smaller coupling efficiency but maximum radiation drive symmetry (DEH). The DEH required the most drive energy and had the lowest capsule drive temperatures; however, it allowed direct control over radiation symmetry to levels of a few percent and the z-pinch, hohlraum,

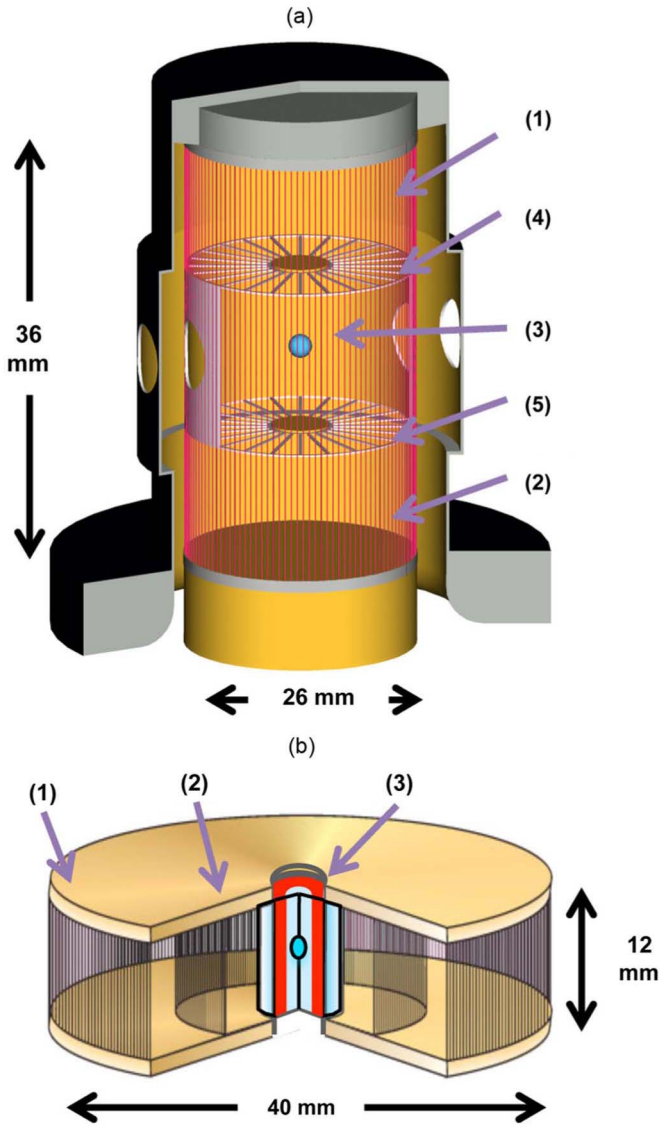

Fig. 2. Comparison of the (a) double-ended hohlraum (DEH) and (b) z-pinch dynamic hohlraum (ZPDH) as fielded on Z. (a) DEH with (1) upper tungsten wire array and primary hohlraum, (2) lower array and primary hohlraum, (3) secondary hohlraum with 2-mm-diameter capsule shown, 3.3 and 4.7-mm-diameter capsules were also used, (4) upper and (5) lower Be spokes. (b) ZPDH with (1) outer tungsten wire array, (2) inner array, and (3) 6-mm-diameter, 14 mg/cm^3 foam target with an embedded 2-mm-diameter capsule. Notional converging shock shown in red.

and capsule system elements could each be independently optimized and studied. Experiments on Z were focused on validation of symmetry control models and understanding the requirements for scaling to ignition and high gain. The DEH was designed for 5-mm-diameter capsules, much larger than the 2-mm capsules being used today on NIF, but ultimately capable of correspondingly larger yields ($>$ 400 MJ) on a future z-pinch driver facility. The ZPDH had the highest coupling efficiency of energy to the capsule, and produced the highest capsule drive temperatures. The drawbacks of this approach included less direct control over drive symmetry and the wire array z-pinch and subsequent target implosion processes were all tightly interconnected. ZPDH experiments on Z were focused on the production and characterization of hot dense capsule cores. The ZPDH had a much lower initial inductance and

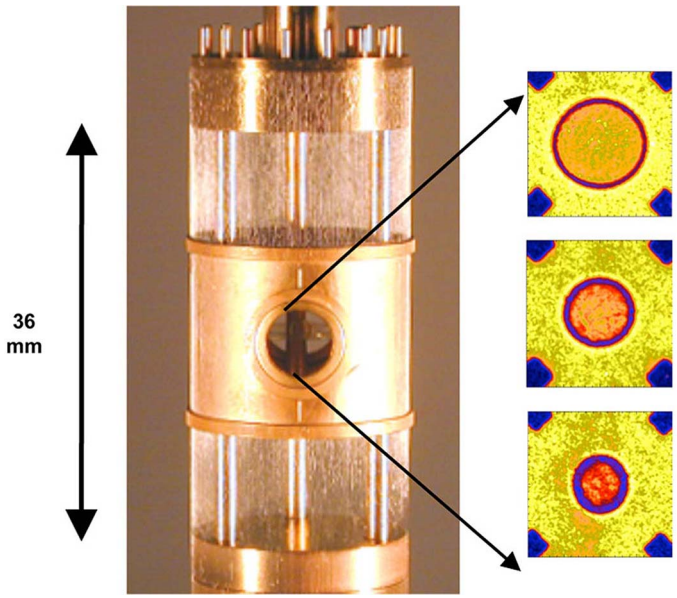

Fig. 3. Double z-pinch wire array with the secondary hohlraum and capsule, and example capsule radiographs, from [24]–[26].

temporal change in inductance, enabling significantly larger (22 MA versus 10 MA) currents to be coupled compared to the DEH. ZPDH experiments for radiation science on the Z facility today are routinely driven at 26 MA in 120 ns, reproducible to within $\pm$ 2% [51].

A. *Double-Ended or Double Z-Pinch-Driven Hohlraum*

The DEH is the most conservative approach to pulsed-power ICF. In the DEH, two cylindrical wire array z-pinches are located in separate primary hohlraums on the top and bottom of a secondary capsule hohlraum. The capsule drive radiation is composed of re-emission from the primary and secondary hohlraum walls. Drive symmetry is tuned by adjusting the overlap of primary and secondary re-radiation, largely through hohlraum geometry, but also through symmetry shields. This arrangement provides the maximum control over radiation drive symmetry and allows no direct line-of-sight between the capsule and pinch. Thus, there is minimal sensitivity to the typical mm-scale-length z-pinch non-uniformities.

DEH experiments were performed on Z with large high-yield-sized hohlraums, as shown in Fig. 2. Time-averaged capsule radiation symmetry of 2% was demonstrated with 2-mm-diameter capsules [24]–[26], compared to 4% with 4.7-mm-diameter capsules [26]. Larger capsules had a significant P4 Legendre mode radiation asymmetry component. Capsule convergence ratios of 14:1 were demonstrated with 2-mm capsules, a record for pulsed-power indirect drive [26]. Fig. 3 shows a double z-pinch wire array and secondary hohlraum with some example capsule implosion symmetry radiographic data [24], [25]. Symmetry was maximized with larger hohlraum case-to-capsule ratios (4 : 1 to 10 : 1). However, the high yield scale size and large case-to-capsule ratio limited drive temperature on Z to about 70 eV, and only about 5 kJ was coupled to the fusion target at the Z scale. This was an energy storage-to-target coupling efficiency E_{target}/E_{store} of 0.044%.

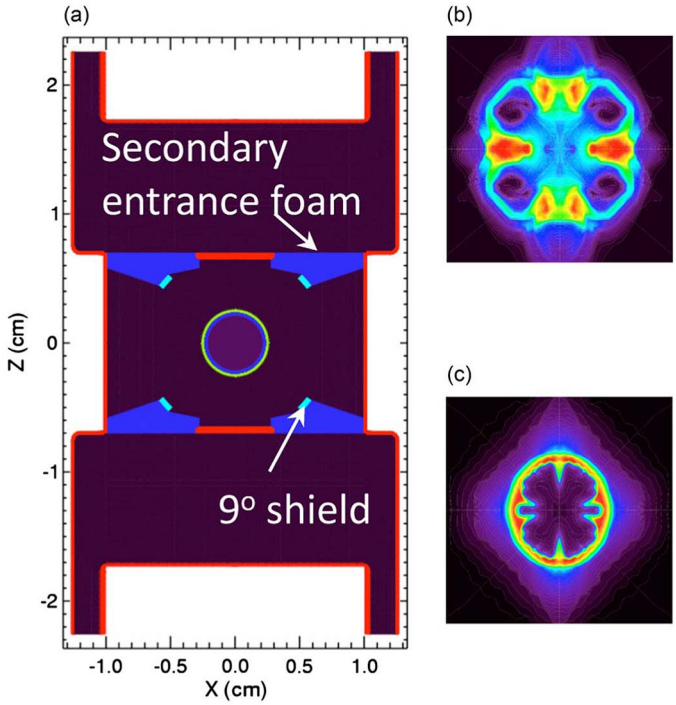

Fig. 4. (a) High yield DEH point design with time-dependent symmetry shields from [27] for simultaneous control of P4 and P6. (b) Capsule implosion without symmetry shields providing a yield of 0.04 MJ. (c) Capsule implosion with symmetry shields providing a full 2-D yield of 460 MJ.

Integrated modeling with 2D-RHD simulations agreed well with experiments and led to a mature DEH design that met radiation symmetry requirements [27]. Symmetry experiments on Z with 4.7-mm-diameter capsules showed a P4 that was sensitive to wall motion based on modeling. Initially, static P4 shields were proposed for experiments. This insight led to time-dependent P4 control techniques [52]. Fig. 4 presents the DEH point design that included a time-dependent P4 burn-through shield developed by Vesey *et al.* [27] that allows control of both P4 and P6. This DEH point design and the accompanying capsule design produced a simulated 460 MJ yield.

These integrated simulations also defined z-pinch source power, energy, and radiation pulse shape requirements. They showed that the DEH point design required two 950 TW, nine MJ z-pinches ($\sim$2 PW and 18 MJ total X-rays). The required radiation pulse from a single pinch is depicted in Fig. 5 [27]. 2D-RMHD simulations of z-pinch implosions treated as 2-D shells suggested that such peak powers and total energies would require currents of 60–70 MA delivered to each pinch in 100 ns. Vesey *et al.* developed an approach to feed these two pinches with a single low-inductance feed, lowering the required stored energy by 30% [27]. Stygar *et al.* developed a 340–400 MJ accelerator design to drive the two pinches in series [53], [54]. The combination of the integrated hohlraum, capsule, and accelerator design provided an engineering or facility gain $Q_E = E_{fusion}/E_{store} > 1$.

An outstanding challenge for this concept is to scale a z-pinch X-ray output from $\sim$120 TW at 1 MJ and 20 MA to $\sim$950 TW at 9 MJ and 60–70 MA. Such scaling would be based on the extrapolation of predictive models, and not an experimental demonstration. Furthermore, the z-pinch must produce

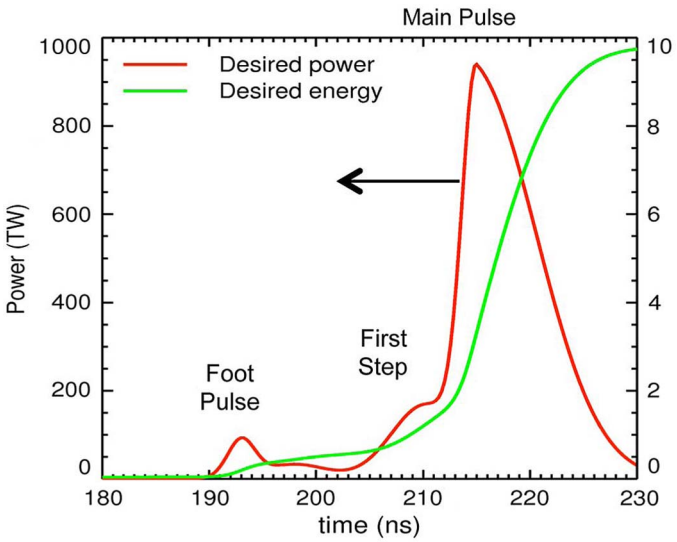

Fig. 5. Three shock z-pinch power pulse required to drive the DEH point design, from [27].

two earlier features in the radiation pulse at precisely controlled amplitudes and times (e.g., see the foot pulse in Fig. 5), to implode the capsule while controlling the shock compression of the DT fuel. To meet these requirements, a significant fraction of the DEH research on Z was spent to develop understanding of the implosion and stagnation dynamics of the compact, 20-mm-diameter tungsten sources. Methods to shape the radiation pulse [27], [55]–[59] were in development. Although progress was being made, as of 2006, there were neither predictive models nor an integrated point design for a z-pinch capable of producing this pulse shape with the requisite peak power and energy.

The experimentally observed X-ray power and energy scaling with current from a variety of wire arrays suggested that ablation physics of high mass arrays might influence the z-pinch physics [60] and lead to a radiated power and energy scaling below the scaling of available magnetic energy ($\mathrm{E_{mag}} \sim \mathrm{I}^2$) for arrays with implosion times of 95–140 ns [61]. For shorter implosion time (80 ns) and lower mass pinches, however, the power and energy scaled closer to I^2 [62]. Comprehensive 3D-RMHD simulations were performed that were validated against all extant compact tungsten wire array z-pinch data [63]. These simulations suggested that the observed scaling below $\sim\mathrm{I}^2$ resulted from current loss in the power feed that was slightly increased for longer implosion times. This remains an open question for experimental validation. The progress in simulations [58], [63]–[68] suggested that we were on a path toward a predictive wire array z-pinch-modeling capability.

During the period of 2006–2008, compact DEH designs were being considered to increase the hohlraum temperature and coupling efficiency. A design was proposed that scaled to radiation temperature of 250 eV and would have required half the drive energy (9 MJ total, compared to 18 MJ). Tamping of hohlraum wall motion, and mode-selective symmetry control would have been more challenging in compact systems. New z-pinch types were being evaluated at universities [69]–[72] and on the Saturn facility [73], [74] to assess compatibility with smaller hohlraums. Entirely new hohlraum concepts were proposed at universities that could significantly improve the coupling efficiency for indirect drive [69], [73].

B. Z-Pinch Dynamic Hohlruam

The ZPDH dramatically increases the capsule coupling efficiency compared to the DEH. A nested tungsten wire array is imploded onto a CH foam cylinder containing the capsule. A rapid ($\sim$30 cm/μs), strongly radiating, symmetric, converging shock produced in the CH foam is the hohlraum X-ray source [18], [20]. The imploding tungsten z-pinch plasma confines the radiation, and the radiation temperature rises dramatically as the pinch both implodes and acts as a moving hohlraum wall. As the implosion proceeds, the hohlraum case-to-capsule ratio decreases, resulting in a more demanding environment to control the radiation symmetry.

Diagnosing the capsule inside an imploding z-pinch was challenging. The ZPDH imploded capsules at peak temperatures of $>$ 200 eV. The temperature when the capsule reached half of its initial radius (thus absorbing only 25% of the available flux compared to its initial size) is called the effective radiation temperature and was estimated to be $\sim 170 \pm 10$ eV [18], [19]. This intense drive produced hot, dense imploded cores with measured electron temperatures of 1 keV [16]. More than 40 kJ was absorbed by 2-mm-diameter fusion capsules with this concept [21], [22], corresponding to an energy storage-to-target coupling efficiency of $\mathrm{E_{target}}/\mathrm{E_{store}}$ of $> 0.35\%$. This was the largest energy coupled to an indirect-drive target at the time and was $8X$ higher than the DEH. We estimate that a factor of several increase in total coupling efficiency for the ZPDH resulted from the larger current delivered to the ZPDH compared to the DEH.

Fig. 6 presents the dynamic hohlraum electron temperatures as derived from spectroscopy of Si dopants included in the $\mathrm{CH_2}$ foams [21], [22]. Based on these data, the effective X-ray energy in the dynamic hohlraum was more than 180 kJ. Such data provided a mature understanding of the dynamic hohlraum energy balance [75]. Neutron yields of $2 - 4 \times 10^{11}$ were produced with this concept, record neutron yields for an indirect-drive capsule at the time. Measurements of the hot spot equator and pole dimensions suggest (time-integrated) radiation symmetry with a P2 of $< 6\%$ [19]. Some control over symmetry was demonstrated by variation of the capsule thickness [19] or ablator material. The capsules were, however, designed to ablate all the target material before the end of the drive pulse.

Progress was also made on integrated high fusion yield target designs for the ZPDH. Preliminary designs suggested that a single 60 to70-MA ZPDH could reach target yields of $\sim$500 MJ [76], [77]. Such a driving current would require less than half the stored facility energy of the DEH, or $<$ 130–200 MJ, providing an engineering gain $\mathrm{Q_E} > 2$. However, radiation symmetry modeling of these designs needed improvement. Updated designs to improve symmetry and provide radiation pulse shaping would likely have required increased drive energy.

X-ray radiographs from dynamic hohlraum tests [78], [79] at 6.151 keV are shown in Fig. 7. In these experiments, a 2.5-mm-diameter Ge-doped plastic CH capsule was embedded inside a

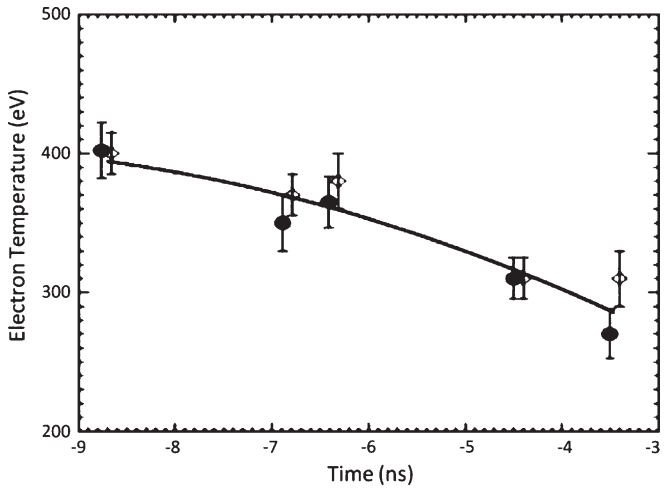

Fig. 6. Time-dependent electron temperature of the radiating shock in the dynamic hohlraum, from [21], [22].

6-mm-diameter, 14 mg/cm^3 CH_2 foam. The foam and capsule were placed on the axis of two nested tungsten wire arrays with a total wire array mass of 3.2 mg/cm. In Fig. 7(a), the majority of the tungsten mass has reached the outer boundary of the foam, and an unperturbed image of the capsule can be seen. In Fig. 7(b), the tungsten shell surrounding the capsule has started to become optically thick to the 6.151 keV backlighting X-rays. The capsule size is about 2.13 mm horizontally and 2.31 mm vertically, indicative of distortion at this early time due to equator-hot asymmetry of the dominantly cylindrical radiation drive. The capsule has only converged by about 11% at this time. The Magneto-Rayleigh Taylor (MRT) instability is observed on the imploding z-pinch in Fig. 7(a) and (b). By the time of Fig. 7(c), the capsule is predicted to have nearly converged, but the tungsten shell surrounding it is too optically thick for the capsule to be visible. The ablated mass from the capsule, however, has disrupted the tungsten implosion and causes the bulge seen in the radiograph. Post-processed simulations of this load [78] qualitatively agree with these images and suggest that the self-emission from the capsule implosion is the source of the bright region near the capsule centers, and that the tungsten implosion produces the remainder of the time-integrated self-emission at the top and bottom poles of the capsule, seen in the image. Though useful, these images illustrate the need for higher-photon-energy backlighting sources (to overcome the z-pinch opacity) and time-gated detectors (to eliminate the time-integrated self-emission). These data also underscore the challenge of diagnosing capsule implosions inside imploding z-pinches.

As of 2006, the ZPDH was used to acquire the first data for a tomographic reconstruction of an imploded capsule [16]. Doped foam layers were being considered to provide radiation pulse shaping for the ZPDH [75]. In addition, shimmed capsule ablators were being considered to control capsule implosion symmetry. Simulations indicated the potential to compensate for a constant P2 drive asymmetry as high as 20% and still produce nominal fusion yields (80% of a symmetrically driven capsule) [80]. A prominent ZPDH issue being discussed at that time was to assess possible mm-scale length radiation non-

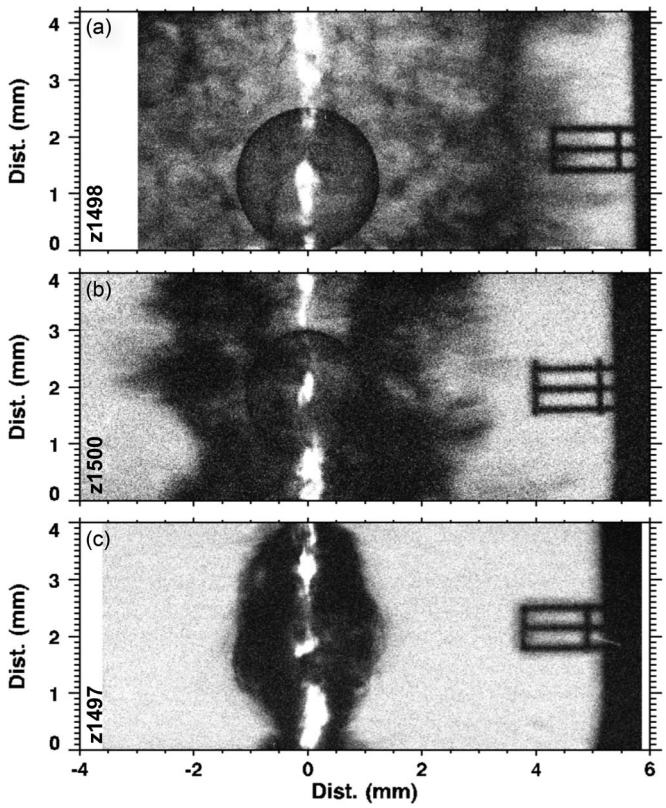

Fig. 7. X-ray radiographs of a 2.5-mm Ge-doped plastic ICF capsule inside of a dynamic hohlraum at 6.151 keV from [78] at (a) $t = -11$ ns, (b) $t = -6$ ns, and (c) $t = -1$ ns with respect to the peak of the radial soft X-ray emission. The hohlraum temperature in part (a) is about 40 eV, in part (b) about 80 eV, and part (c) near peak drive. The bright-white regions at r $= 0$ are images of the time-integrated 6.151 keV self-emission produced by the tungsten implosion and the capsule implosions.

uniformities that may have resulted from opacity variations in the imploding tungsten z-pinch due to the MRT instability.

IV. Direct-Magnetic-Drive Pulsed-Power Fusion Concepts

A. Direct-Magnetic-Drive With Magnetic Pressure

Although the refurbished Z could provide 2-3X more energy coupled to indirect-drive capsules, such an increase would only provide marginal increase in the ability to do important fusion science. The utility of direct magnetic pressure to drive interesting conditions in direct MDI of fusion targets is provided by a simple estimate for the magnetic pressure in MBar:

$$P_{mag} = \frac{B^2}{2\mu_o} = 105\left(\frac{I_{MA}/26}{R_{mm}}\right)^2 [MBar]. \qquad (7)$$

Thus, if the peak Z current of 26 MA can be brought to a radius of 1 mm, a pressure of 105 MBar would result.

This can be compared with the radiation ablation pressure provided by an intense X-ray radiation field in a hohlraum. The rocket effect of plasma ablated from the surface of the capsule by the radiation provides a pressure given by

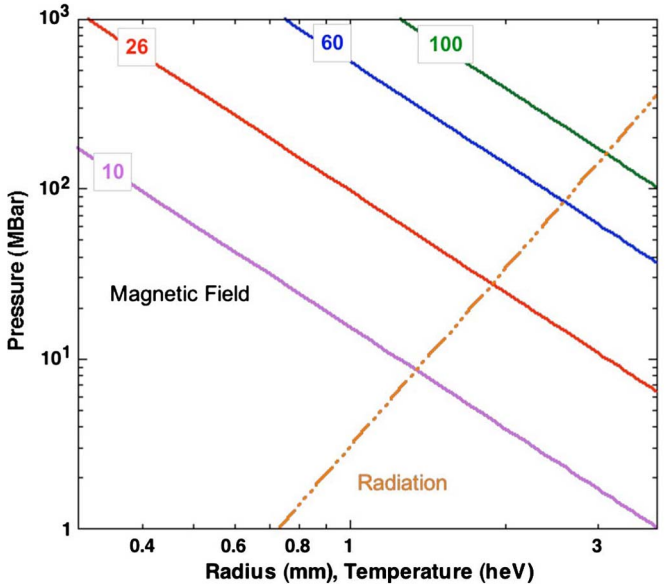

Fig. 8. Comparison of magnetic pressure as a function of radius, and radiation ablation pressure as a function of radiation drive temperature, from (7) and (8). The pressure is in MBars, the radius in mm, and the temperture in hundreds of eV. Solid lines are for magnetic pressure, increasing as $(\mathrm{I/R})^2$. The broken line is for radiation pressure increasing as $\mathrm{T}^{3.5}$.

Equation (8), where P is in Mbar and the temperature is in hundreds of eV [41]:

$$P_{rad} = \frac{(2/5)(1-\alpha)\sigma T^4}{C_s} = 3T_{heV}^{3.5}[MBar]. \qquad (8)$$

The values in the right-hand side of the equation are for a plastic shell. A peak drive temperature of 300 eV (or 3 heV, as on the NIF) provides a capsule drive pressure of 140 MBar. The drive pressures produced on the Z and the NIF may therefore be comparable. This will depend on bringing the current to small radius.

Fig. 8 compares the magnetic pressures that would be provided by imploding peak currents of 10, 26, 60, and 100 MA to various radii with the radiation pressures produced by different hohlraum temperatures, from (7) and (8). Magnetic drive pressures (at $\mathrm{R} < 2$ mm) are significantly larger than the radiation ablation pressures for conditions reachable on the Z facility ($\mathrm{T_{rad}} \leq 200$ eV). Energies delivered to the targets by work done by the magnetic pressure over the implosion are also correspondingly higher. Since the magnetic pressure increases during implosion, the energy delivered to a magnetically imploded system increases as $\sim ln(Cr)$, where Cr is the convergence ratio of the target. Conversely, the energy delivered in a radiation ablation-driven system decreases as Cr^{-2}. On a future facility, imploding 60 MA to a radius of 1 mm would provide a drive pressure of more than 500 MBar, equivalent to a drive greater than 300 eV. Higher drive pressures could lower the energy required for ignition in cylindrical targets as it does for X-ray-driven spherical implosion [81].

Though the Z accelerator can provide drive pressures of order 0.1 Gbar, achieving or exceeding laboratory fusion breakeven will require fuel stagnation pressures of 1–100 Gbars. Such high stagnation pressures can only be achieved transiently through the acceleration and rapid assembly of fusion fuel. Furthermore, the pressure must be delivered quickly to heat the target to overcome plasma heat losses, and this requires a fast implosion velocity of 20–40 cm/μs. Attaining these velocities at realistic convergence ratios, in a configuration stable enough against implosion instabilities will be challenging. The fuel must also be compressed to sufficient ρR. Fuel ρR increases more slowly with convergence ratio for cylindrical implosions ($\rho R \sim 1/r$) than for spherical implosions ($\rho R \sim 1/r^2$). Cylindrical pulsed-power targets imploded in 100 ns will require additional target design elements to compensate for the slower increase of ρR and slow implosion velocity. As discussed, larger delivered energies, larger fuel mass, fuel pre-magnetization and fuel pre-heat are predicted to allow interesting fusion conditions to be attained.

The equation of motion of a liner accelerated by a linearly rising current pulse can be numerically solved to provide the scaling of the liner velocity with key liner and driver parameters (see Appendix A). This solution highlights some of the design choices available for liner implosions relevant to fusion. This scaling is an upper limit since it neglects the decrease of pinch drive current in real-world drivers that result from the increasing inductance of the load relative to the generator. In addition to this reduction in drive current that can be described by a circuit model, the increasing voltages can also be associated with current loss in the power addition section of the pulsed-power generator [82] and possibly also in the power feed to the load [63], [67]. We find that the pinch implosion time is well fit by a simple analytic form to within 1%:

$$\tau_{dI/dt} = 1.72\left(\frac{4\pi^2}{\mu_o}\right)^{1/4}(dI/dt)^{-1/2}\rho_L^{1/4}r_o\left(\frac{2-1/A_R}{A_R}\right)^{1/4}. \qquad (9)$$

In this expression, dI/dt is the rate of rise of the current, r_o is the liner radius, ρ_L is the liner material density, and A_R is the initial liner aspect ratio. The liner aspect ratio $A_R = r_o/(r_o - r_i)$, is the ratio of the liner outer radius to the liner thickness [30]. The liner convergence ratio, $Cr = r_o/r_{final}$ where $r_o(r_{final})$ is the initial (final) radius of the imploding target. This expression was compared to numerical solutions over a range of $4 \leq A_R \leq 20$, $0.1 \leq dI/dt \leq 2$ MA/ns, $10 \leq Cr \leq 30$, and $0.1 < r_o < 1.0$ cm. At a radius of $r_o = 0.3$ cm, the aspect ratios and dI/dt's correspond to liner masses of 25 to 170 mg, and liner thicknesses of 125 to 1000 μm. See Appendix A for a derivation of this result and others below, and the associated plots.

In convenient units:

$$\tau_{dI/dt}[\mathrm{ns}] = 229\,(dI/dt[\mathrm{MA/ns}])^{-1/2}\left(\rho_L[\mathrm{g/cm^3}]\right)^{1/4} \times r_o[\mathrm{cm}]\left(\frac{2-1/A_R}{A_R}\right)^{1/4}. \qquad (10)$$

Slutz *et al.* discussed a MagLIF liner design for Z [30] with $\rho_L = 1.85$ g/cm^3 for Be, $r_o = 0.34$ cm, $dI/dt = 0.25$ MA/ns, and $A_R = 6$, where (9) gives $\tau_{dI/dt} = 135$ ns. Equation (9) agrees well with experiments [35] which used $r_o = 0.345$ cm, $\langle dI/dt\rangle_{25-75\%} = 0.29$ MA/ns, predicting $\tau_{dI/dt} = 127$ ns compared to the measured $\tau_{\mathrm{imp}} = 130$ ns.

We find the following for the peak pinch implosion velocity, using the numerical solution (Appendix A):

$$v_{imp} = 0.9 \left(\frac{3\mu_o^{1/2}}{\pi}\right)^{1/2} (dI/dt)^{1/2} \times \rho_L^{-1/4} \left(\frac{A_R}{2 - 1/A_R}\right)^{1/4} [\ln(Cr)]^{1/2}. \quad (11)$$

In convenient units:

$$v_{imp}[\text{cm}/\mu\text{s}] = 16.4\,(dI/dt[\text{MA/ns}])^{1/2} \left(\rho_L[\text{g/cm}^3]\right)^{-1/4} \times \left(\frac{A_R}{2 - 1/A_R}\right)^{1/4} [\ln(Cr)]^{1/2}. \quad (12)$$

We note that actual velocities from calculations incorporating a circuit model are lower than (11) because of the resulting decrease in dI/dt as the load inductance increases. The implosion velocity is most strongly dependent on the generator's dI/dt. The next two terms (ρ_L, A_R) describe the initial liner parameters. The implosion velocity is weakly dependent on both. Also, note the weak dependence on the Cr. The final two terms (A_R, Cr) determine, in part, the subsequent evolution of the implosion. Both terms have an impact on the robustness of the liner implosion to the MRT instability growth, but this tradeoff is not contained in this description. High A_R liners clearly reach higher implosion velocities (less mass to accelerate), but such liners are more susceptible to the MRT instability. 2D-RMHD simulations suggest that thicker liners (lower A_R) could allow sufficient liner ρR to remain intact at stagnation to compress and inertially confine the fusion fuel [30], whereas thinner liners (higher A_R) may be too disrupted. The MRT instability is believed to be one of the largest threats to the success of pulsed-power direct-driven fusion concepts.

Low liner densities are preferable for achieving higher velocities for fixed mass (e.g., for a fixed implosion time), while maintaining compatibility with the use of thick liners (low A_R) that may be more robust to the MRT instability. The target design of [30] used Be. If instead of a Be liner ($\rho_L = 1.85$ g/cm^3), we use lithium ($\rho_L = 0.535$ g/cm^3), the implosion velocity would be increased by 36%, for the same A_R and Cr. Li could also allow a lower A_R and/or Cr for a given implosion velocity. For example, Li could allow equivalent implosion velocities at an A_R of 3 with a Cr of 10:1, which may be favorable for MRT. By contrast, moving to Al ($\rho_L = 2.7$ g/cm^3) would decrease the implosion velocity by 9%. Safety, machinability, strength, and other constraints may ultimately dictate the best liner material, but we are currently investigating all of these options.

The strongest variable affecting the implosion velocity is the generator dI/dt. Implosion velocities of 40 cm/μs, comparable to NIF capsules, could be obtained for $A_R = 6$ beryllium liners at dI/dt's of 2 MA/ns. This is beyond the reach of present technology. Higher dI/dt's require higher voltages and electric fields. For proposed architectures (see Section VI), a higher dI/dt is accompanied by an increase in the facility inductance required to manage the higher electric fields and prevent breakdown. This results in a rapid increase in the required electrical power, $P_{elec} \sim (dI/dt)^{5/3}$ and therefore increases the system size and cost [53], [54], nonlinearly. VanDevender *et al.* [83]–[85] propose new technologies and system architectures to reach these current risetimes. Switches, such as the exploder switch [86], might also be able to increase the dI/dt from a given generator by a factor of 2.5. If the dI/dt on Z could be increased by a factor of 2.5 (to 0.75 MA/ns), implosion velocities approaching 30 cm/μs might be possible, sufficient for target self-heating. Next generation pulsed-power generators with dI/dt's of 70 MA in 120 ns (0.6 MA/ns) [53] [54] would allow implosion velocities of about 25 cm/μs. A_R of 20 would permit implosion velocities of 35 cm/μs at these dI/dt's. Such target designs will require improved understanding of the MRT instability and its dependence on A_R, Cr, dI/dt, and other conditions such as surface roughness and other material properties. These issues are subjects of active investigation [32]–[35], [37].

The use of pulsed-power-generated current and its magnetic field to directly compress fusion fuel within a liner, using the Lorentz force, has been proposed for many years [87]–[96]. Other target design elements are incorporated to overcome the limitation on implosion velocity imposed by (10) and (12). The implosion velocities of these proposed systems are too low for significant self-heating of the plasma, so that an independent method of forming and injecting hot plasma is sought. As a result of low implosion velocities (< 20 cm/μs) and long implosion times (> 1 μs), these concepts also include the use of a magnetic field to reduce electron thermal conduction losses from the fusion fuel. The slower implosion times require magnetically confined and pre-heated plasma with closed field lines to trap heat flow in all directions. The proposal to use magnetic fields to reduce electron thermal conduction losses in fusion fuel has a long history [97], [98], and has had experimental demonstration [99]–[103].

Lindemuth and Kirkpatrick [47] showed that significant gain could be obtained with implosion velocities below 1 cm/μs using magneto-thermal insulation, even with low initial fuel densities ($\sim$1 μg/cm^3). Since the electrical powers required to implode a pinch are proportional to the kinetic power of the pinch (which is $\sim$v^3), the electrical power and cost of such a pulsed-power system is significantly reduced. Reference [92] suggests that such magneto-inertial fusion concepts are intermediate in the assembled fuel densities required between magnetic confinement and inertial confinement. Fusion experiments in this intermediate class have a much lower cost and might be done on intermediate scale facilities, such as the Atlas [104] or Z pulsed-power generators [28], [29]. Significant effort has been put into these ideas over the last few years [91], [95], [96] resulting in a concept to use a liner implosion on the Shiva Star [105] facility at 0.5 cm/μs to compress a field-reversed-pinch injected into the liner. Such configurations are ultimately limited to gains of about 10 because of the nature of volumetric burn [44]. Preparatory work for this concept has demonstrated target convergence ratios of 12–15:1, a record for pulsed-power direct drive [91].

Quasi-spherical direct-drive implosions to achieve larger increases in fuel density with target compression ($\sim 1/R^3$ instead of $1/R^2$ in cylindrical geometry) have been proposed [83]–[85], [106], [107]. Nash *et al.* [106], following earlier work by Degnan *et al.* [107] and others, suggested using single (or nested) quasi-spherical implosions in 100 ns. The goal was

to achieve higher ρR's than in cylindrical geometry at Cr of 12–24:1, without pulse shaping or cryogenic fuel, and with implosion velocities (14–30 cm/μs) that were suggested to be high enough for adequate self-heating of the hot spot. However, the designs use high aspect ratio targets ($A_R = 20 - 120$) to achieve high implosion velocities, and thus would be more susceptible to the MRT instability than implosions of lower A_R liners.

VanDevender *et al.* proposed [83] quasi-spherical targets with cryogenic layers imploded in 40 ns. Extensive simulations of these targets indicated they could achieve high ρRs and high implosion velocities (> 35 cm/μs) for rapid plasma self-heating, ignition and fusion gain. These targets required an A_R of 21 and a Cr of about 13. However, this approach requires larger $dI/dt (\geq 1.5$ MA/ns) than existing multi-MA pulsed-power technology has demonstrated ($\sim$0.3MA/ns). Equation (11) suggests that at dI/dt's of > 1 MA/ns, this A_R and Cr result in implosion velocities of > 40 cm/μs. Several technologies have been proposed [84], [85] to achieve such current rise rates. A significant research program to develop this capability would be required before progress could be made with this target approach.

Slutz and Herrmann *et al.* show [30] that the use of fuel pre-heating and fuel magnetization can allow relatively slow liners (10 cm/μs) with target designs possibly resilient to MRT ($A_R = 6$) to achieve significant fusion yields using existing pulsed-power technology ($\leq$ 0.3 MA/ns) on the 100-ns drive Z facility. Indeed, (11) suggests that under these conditions, the peak implosion velocities of magnetically driven liners on Z are no more than 20 cm/μs. The next section discusses our plans to evaluate MagLIF. As we make progress in our understanding of the MRT and its dependence on liner and driver parameters (A_R, Cr, and dI/dt), other target designs can be proposed and evaluated.

B. MagLIF

The MagLIF concept and phases are shown in Fig. 9 [30]. The liner is initially filled with gaseous D_2 or DT fuel [Fig. 9(a)]. The system is magnetized with an axial magnetic field B_z [Fig. 9(a)] produced by an independent coil system (see Fig. 12). The field is established slowly enough over several ms to allow it to fully penetrate all the hardware, including the target. Current from the Z generator is delivered, producing a B_θ field to implode the target [Fig. 9(a)]. To pre-heat the fuel, the multi-TW, multi-kJ, 527-nm Z-Beamlet laser [108] co-located with the Z facility can be used (see Fig. 10). After the start of the implosion, a 10 ns pulse from the Z-Beamlet laser is directed into the liner and pre-heats the fuel to 250–500 eV [Fig. 9(b)]. The implosion continues to convergence ratios of 20 : 1, adiabatically heating the fuel, compressing the B_z to $>$ 50 MGauss fields, which hinders electron thermal conduction loss to the liner wall.

Integrated MagLIF target designs predict that DT fusion yields of order 100 kJ may be possible on Z at peak drive currents of about 27 MA, with an initial axial magnetic field of 30 Tesla, and with about 6 kJ of Z-Beamlet laser pre-heat energy. This yield would represent *scientific breakeven* where the fusion energy output (E_{fusion}) equals the energy invested in heating the fuel (E_{fuel}). This is sometimes represented by the condition $Q_{HS} = 1$, where $Q_{HS} = E_{fusion}/E_{fuel}$ is the gain of the hot spot. Scientific breakeven, to our knowledge, has not been achieved in any fusion system to date.

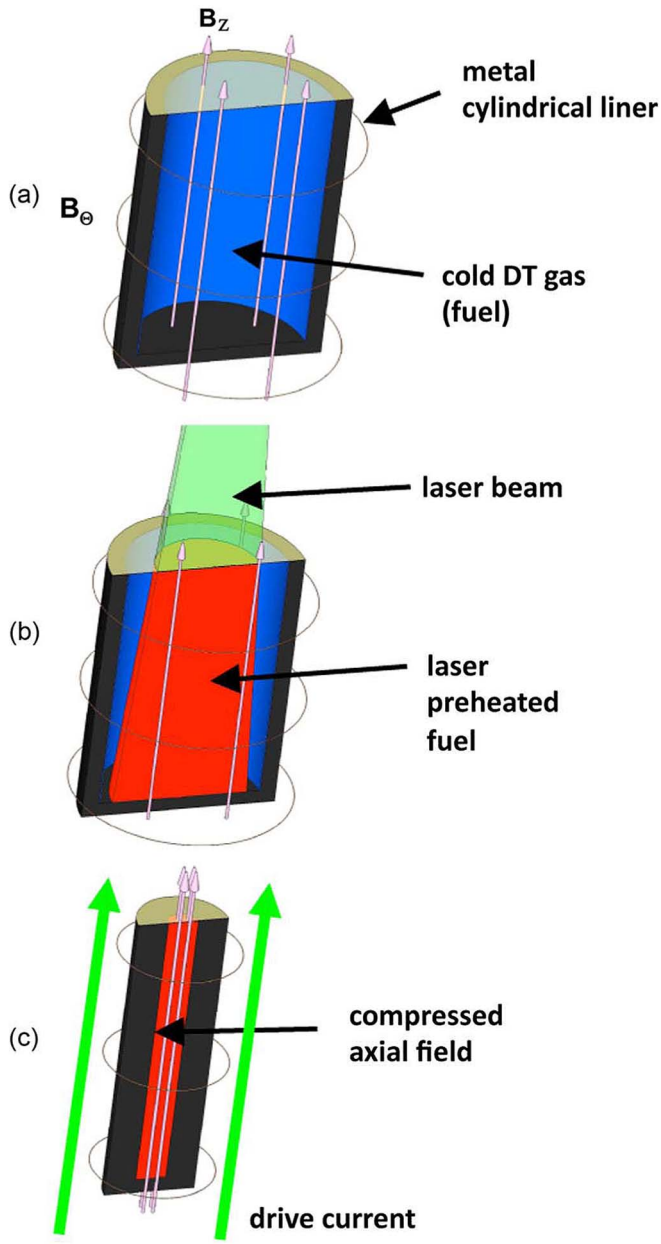

Fig. 9. Phases of the MagLIF concept, showing (a) axial pre-magnetization phase, (b) laser pre-heat phase, and (c) magnetically driven liner implosion and flux compression phase, described more fully in the text.

Such fusion yields were never envisioned in designs for any indirect-drive concept on Z. The 100 kJ predicted DT fusion energy yield is equivalent to 3.5×10^{16} neutrons. Equivalent yields from D_2 MagLIF implosions would be of order 4.4×10^{14} neutrons (80X lower). Such an output could be considered a "*scaled scientific breakeven*" condition. For comparison, the maximum experimentally measured D_2 yields from the indirectly driven ZPDH were of order $2 - 4 \times 10^{11}$ [17], [19], a factor of 10^3 lower. The maximum *predicted* neutron yields for the DEH were of order $10^8 - 10^9$. Although both the ZPDH and DEH designs could be improved, clearly the relative

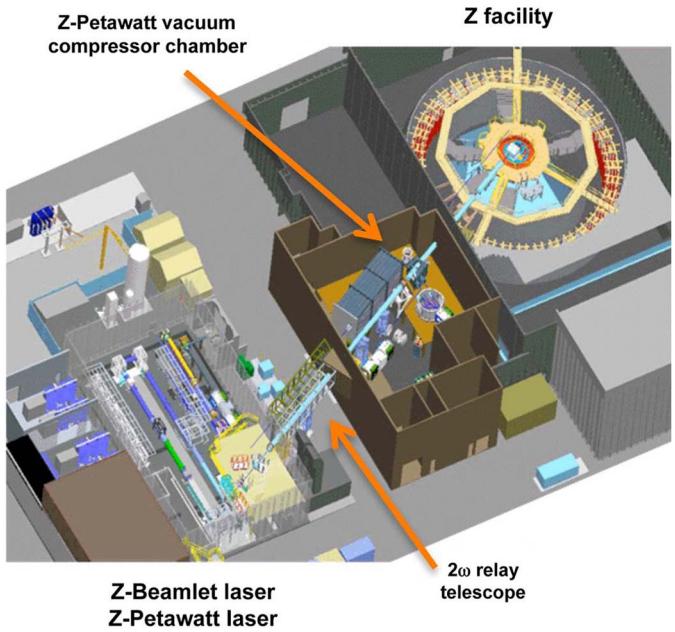

Fig. 10. National Nuclear Security Administration experimental facilities at Sandia National Laboratories showing the layout and integration of the Z pulsed-power generator, and the Z-Beamlet, and Z-Petawatt laser facilities.

potential of MagLIF is noteworthy for near-term experiments on Z, and for scaling to future high fusion yield facilities. Much work remains to be done to evaluate the potential of this concept.

A high-gain version of MagLIF has been designed that utilizes a dense cryogenic fuel layer as a target design element [31]. This design may allow GJ fusion yields on a future 60 MA pulsed-power facility. This yield exceeds our predictions for any of the previously studied indirect-drive concepts at such currents, largely because of increases in coupling efficiency to targets (10–150X). The target coupling efficiency is the absorbed energy by the target normalized to the energy stored in the driver. The absolute target absorbed energy increases by 10-50X. High gains are of great utility to national security missions, and to progress in inertial fusion science. Higher efficiency and higher gains may translate into more compelling (lower cost and complexity) fusion reactor designs.

The six critical characteristics or design elements for MagLIF targets and the related goals are summarized in Table I. We are building toward the first integrated experiments with these elements (liner dynamics, liner stability, magnetized and pre-heated fuel, fusion diagnostics) in 2013. Near-term experiments will be conducted with pure D_2 fuel, at peak drive currents of 15–20 MA, magnetic fields of 7 Tesla, and laser energy of 2 kJ. These conditions will be increased to those required for tests of scaled scientific breakeven (27 MA, 30 T, 6 kJ) over the next five years. Simulations indicate that the additional design elements may reduce requirements on fuel ρR for significant yield from 300 mg/cm^2 to 30 mg/cm^2, reduce the requirements on implosion velocity from 35 cm/μs to 10 cm/μs, and reduce the requirements for fuel convergence ratio from 35 : 1 to 23 : 1. An extensive campaign of integrated implosion experiments and experiments focusing on selected physics issues will be carried out over the next five years to validate these simulations and MDI target design elements.

Reaching yields of $\sim$100 kJ will require DT fuel. At the moment, the Z facility does not have authorization to use DT fuel. We are developing the safety basis, system pre-conceptual designs, and individual technologies necessary to utilize DT safely on Z. Once we validate the MagLIF concept with D_2 fuel, we will consider the costs and benefits for the utilization of DT. Achievement of a significant fraction of scaled scientific breakeven ($\sim$30% or a DD neutron yield of about 10^{14} neutrons) would represent a high level of target physics understanding with remaining uncertainties and is suggested as a criterion to make investments in the systems for handling of Tritium on Z. The use of DT fuel would accelerate the understanding of fusion conditions in the hot spot through the use of advanced DT neutron diagnostics developed for the NIF [45].

There are a number of issues that must be studied for the MagLIF concept. There are general issues that are similar to conventional ICF target experiments, such as: instability growth, pusher-fuel mix, implosion velocity and convergence ratio, and pusher adiabat [41]–[44]. The way these issues are realized for MagLIF will, however, be unique. In addition there are a number of new issues that arise due to the new nature of the implosion, of the fusion fuel production, heating, and reliance on the modification of particle transport and confinement. Issues that must receive systematic study include:

- Initiation of current flow and plasma formation on liner surface.
- MRT instability growth (analogous to RT instabilities in capsules).
- Coupling of magnetic flux between the pulsed-power generator and the target.
- Laser heating of fusion fuel, plasma lifetime, and uniformity, particularly in the presence of a magnetic field, and with end losses of pre-heated plasma.
- Efficacy of magnetic fields for suppressing electron thermal conduction loss during an MDI.
- Flux compression and magnetic flux transport through a plasma liner.
- Efficacy of high magnetic fields for inhibiting alpha particle loss from the hot spot.
- Deceleration Rayleigh-Taylor instabilities and mix during stagnation.

These issues, and others, will be studied in focused and integrated experiments.

The MagLIF design with gas fill [30] and with Be targets at $A_R = 6$ does not show a measureable signature of alpha particle heating until currents of 35–45 MA. At 40–50 MA, sufficient fuel density, compressed magnetic flux, fusion yield, and liner density are achieved to produce gains of up to 10, with a volume burn [44]. However, other target designs may be possible that allow significant alpha particle heating at lower currents. Work is ongoing to optimize the MagLIF target design for currents of order 20 MA. Cryogenic layers may permit measureable signatures of alpha particle heating at drive currents of 30 MA [31]. The alpha particle slowing in this cryogenic fuel layer are predicted to produce about 1 GJ yields and gains of up to 100 at a 60 MA drive current, and about 10 GJ yields and gains of 1000 at 70 MA [31].

Experiments on liner implosions and initiation that are relevant to MagLIF have begun. Liner initiation and plasma

TABLE I
CRITICAL DESIGN ELEMENTS FOR MagLIF TARGETS AND GOALS

Element	Goal
Cylindrical target	• Simplicity of experiments and implosion physics • Ease of target fabrication • Best diagnostic access • Compatibility with purely axial magnetic field topology • Access to interior of liner for fuel pre-heat • Short pulse length (100 ns) allows acceptable end loss • Simpler cryogenic layer formation, eventually
Direct magnetic drive	• Large targets and large fuel volumes • Increase driver coupling efficiency and target energy by eliminating: conversion efficiency of magnetic energy to x-rays coupling efficiency of x-rays to hohlraums conversion efficiency of x-rays to capsule kinetic energy
Pre-magnetized gaseous D_2 or DT fuel	• Mitigate electron thermal conduction heat losses from the plasma • DT plasmas will increase yield and neutron diagnosis of fusing plasmas at considerable increase in complexity for safe handling of Tritium
Flux compression of initial Bz field by a factor of ~10^2–10^3	• Mitigate thermal conduction losses from preheated fuel to liner • Reduction of liner implosion velocity requirement • Reduce hot spot ρR requirements, at some scale
Pre-heating of the pre-magnetized DT fuel with the Z-Beamlet laser	• Z-Beamlet is available at Z and possibly simpler than other methods of introducing a pre-heated plasma • Reduces the requirements on plasma self-heating which: reduces the liner implosion velocity requirement reduces the liner convergence ratio requirement is compatible with the Z I-dot
Cryogenic fuel layers	• Provide a cold compressed fuel layer in contact with the hot spot, allowing radial burn and high fusion yields

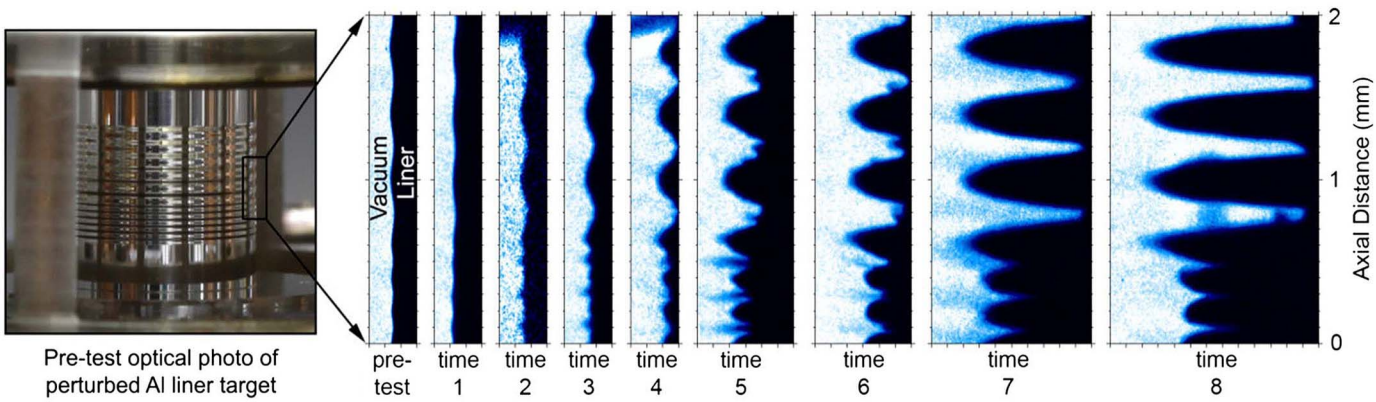

Fig. 11. MagLIF Al liner implosion radiography data on the growth rate of the Magneto-Rayleigh Taylor instability from [32] and [33].

formation physics has been studied in many recent experiments [37], [109]–[112]. The importance of the electrothermal instability in possibly providing an initial seed for subsequent MRT instability growth has been highlighted recently [37]. The MRT instability growth has been studied extensively [32]–[35], [113]–[117]. Fig. 11 presents MRT instability growth measurements using 6.151 keV X-ray radiography of Al targets [32], [33]. Sinars *et al.* [32], [33] show excellent agreement between these data and 2D- and 3D-RMHD simulations for MRT growth of sinusoidal perturbations that had initial amplitudes of 5% of the initial wavelength. McBride *et al.* [35] have studied the MRT growth from random machined surface roughness and non-random machining tooling marks on Be liners, also showing excellent agreement with 2D- and 3D-RMHD simulations. These platforms offer great promise for determining the limits of and tradeoffs for A_R and Cr against liner instability growth.

MDIs of cylindrical liners also have tangible synergies with dynamic materials. Be liners have been compressed isentropically and used to infer the Be EOS to more than 6 Mbar [38], [39]. Precise current pulse shaping was used to avoid forming a shock in the liner. Using precision current pulse

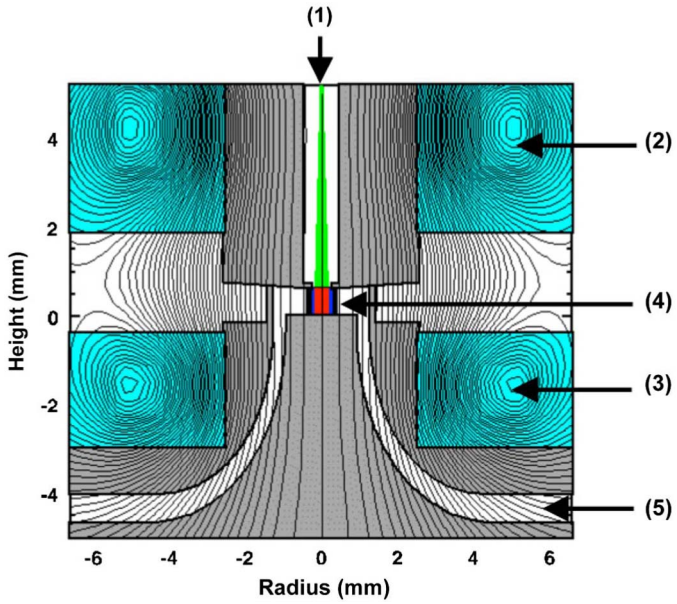

Fig. 12. Magnetic field coil subsystem for MagLIF showing (1) pre-heat laser access, (2) upper coil, (3) lower coil, (4) liner target, and (5) power feed. The upper and lower coils are separated to provide full diagnostic access.

shaping techniques on Z, Be liners have been imploded to convergence ratios of about 5 while maintaining the innermost portion of the liner as solid/liquid [38], [39]. Such techniques may find application to fusion experiments to implode the liner and fuel on a lower adiabat, but more work is required. The shock in the liner on non-pulse-shaped experiments has been imaged with radiography [40]. Liner implosion dynamics will remain an active area of research for several years as we gain understanding and confidence in our modeling.

In addition to liner implosion physics, we are making progress in implementing the magnetic field and pre-heat capabilities required to test MagLIF. Rovang *et al.* have demonstrated an independent coil system capable of 7–10 Tesla axial magnetic fields over a several cm^3 volume with a rise time of a few ms [118]. The coil design includes full side-on diagnostic access and axial access for laser pre-heating. Capacitor banks are being integrated into the Z facility in 2013 that will provide sufficient stored energy to reach 30 T with an appropriate coil. We plan the first magnetized experiments during calendar year 2013 to assess impact of the applied field on current loss in the power feed and to directly measure the flux compression. Fig. 12 shows a conceptual design of the coils and liner, highlighting the field geometry.

The target fill pressures, laser intensities, and laser energies required for MagLIF are similar to conditions previously investigated in preparation for NIF experiments [119]. The previous experiments were benchmarked against standard ICF codes such as Lasnex [120] and HYDRA [121]. We are currently using these codes to design independent experiments to validate the pre-heat plasma temperature increase using the Z-Beamlet [108] laser at the scale for MagLIF (Fig. 10). We note, however, that many of the plasma conditions created during the various stages of MagLIF can be scaled to smaller sizes using dimensional arguments [122]. This may allow university facilities such as the Omega laser [100]–[103] and others, to test key physics questions associated with pre-heat and compression stages.

MagLIF-specific target designs and pertinent engineering and physics issues will be evaluated on the roadmap provided in Table II over the next five years. We are developing a multi-year program plan to deploy these capabilities, to explore the scientific issues enumerated above, and to validate pulsed-power-driven target designs. Although these designs primarily employ gas fill, cryogenic target designs and cryogenic fill systems have been developed and fielded on Z that are compatible with advanced target designs on the path to ignition and high yield. Cryogenic fuel layers will be integrated with these experiments after 2016.

V. Comparison of Indirect-Drive and Direct-Drive Target Designs for 100-ns Pulsed-Power Drivers

There are a number of metrics for comparison of indirect and direct-drive targets. We consider complexity, efficiency of delivery of energy, fusion yields, hot spot gain, and the potential engineering gain of a facility.

DEH and ZPDH experiments require considerably more complex target fabrication and assembly. Fig. 13 provides a scaled comparison of the DEH and the MagLIF targets. The steps include fabrication of a spherical ICF target with cryogenic fuel layer, capsule mounting in the secondary hohlraum or in the foam target, and assembling the wire array(s) around the capsule hohlraum. MagLIF targets are much simpler. These cylinders are machined with diamond turning. The top MagLIF target in Fig. 13 is Al, the bottom Be. A subject of ongoing experiments is to understand the impact of the initial surface roughness on the evolution of the MRT. The (shiny) Al MagLIF target has an RMS surface roughness of 20 nm, the bottom Be a roughness of 200 nm. Neither target has been polished; these are the best surfaces that can presently be produced with either material via diamond turning, without polishing.

We describe the efficiency of delivery of energy from the driver energy storage to the fuel by breaking it into three or four steps encompassing different stages of the process:

- The driver efficiency, $\eta_{\rm d} = {\rm E}_{\rm load}/{\rm E}_{\rm store}$, is the conversion efficiency of electrical energy stored in the capacitors in the pulsed-power generator into the magnetic energy delivered to implode the z-pinch load.
- The X-ray conversion efficiency, $\eta_{\rm x} = {\rm E}_{\rm xray}/{\rm E}_{\rm load}$, is the conversion efficiency of load magnetic energy into useful X-rays that are emitted in a shaped radiation pulse meeting the capsule requirements. This step is not applicable to direct drive, e.g., $\eta_{\rm x} = 1$.
- The target coupling efficiency, $\eta_{\rm c} = {\rm E}_{\rm target}/{\rm E}_{\rm load}$, (or $= {\rm E}_{\rm target}/{\rm E}_{\rm xray}$) is the efficiency of coupling either the magnetic energy delivered to the load into the thermal and kinetic energy of the imploding target or coupling the z-pinch X-rays to the thermal and kinetic energy of the capsule. $\rm E_{target}$ is the total energy absorbed (thermal and kinetic) by the target.
- The fuel coupling efficiency, $\eta_{\rm f} = {\rm E}_{\rm fuel}/{\rm E}_{\rm target}$, is the efficiency of coupling the energy absorbed by the target into the fuel kinetic energy. The fuel kinetic energy is

TABLE II
MagLIF TARGET EVALUATION ROADMAP

Timeline and comments	Capabilities Needed	Issues
2013-2014: Initial Integration	16 MA target current 2-4 kJ laser pre-heat 10-20 T B-field D_2 gas fuel	Impact of magnetic field on current coupling efficiency, and on liner dynamics and liner stability, flux compression efficiency, pre-heat plasma temperature, lifetime and heating uniformity, liner convergence ratio and implosion velocity
2015-2016: Scaled D_2 Performance	20 MA target current 6 kJ laser pre-heat 20-30 T B-field D_2 gas fuel	Pre-heat plasma characteristics, impact of B on liner stability, liner convergence and implosion velocity, heating of magnetized plasmas, stagnation plasma parameters and fusion target performance
2016: Cryogenic Fuel Layers	D_2 cryogenic target designs	Target engineering, possibly increased yield resulting from radial burn of cryogenic fuel
2017: Scaled Breakeven	27 MA target current D_2 gas and cryogenic fuel	Stagnation plasma parameters and fusion target performance
2018: Full DT Performance	27 MA target current DT gas fuel	Stagnation plasma parameters and fusion target performance

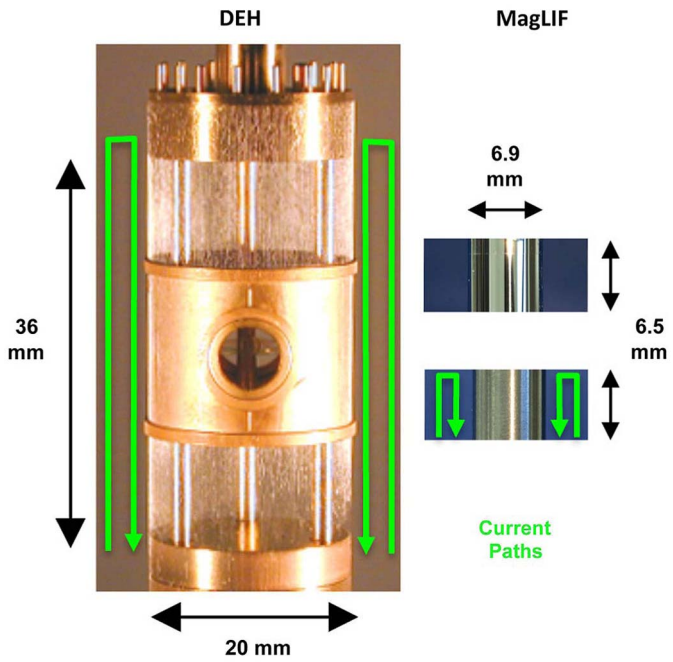

Fig. 13. Scaled comparison of the DEH and MagLIF targets. Al MagLIF target on top, Be MagLIF target on bottom.

converted into fuel thermal efficiency with high efficiency, at fuel stagnation.

The total efficiency of coupling driver energy to the fuel is the product of these four efficiencies: $\eta_{\rm t} = \eta_{\rm d} * \eta_{\rm x} * \eta_{\rm c} * \eta_{\rm f} = {\rm E_{fuel}}/{\rm E_{store}}$. There are significant improvements in $\eta_{\rm x}$, $\eta_{\rm c}$, and $\eta_{\rm f}$ for direct drive compared to indirect drive. The increase of energy delivered to the targets increases the fusion yield possible on a fixed size driver, and also results in higher yields

TABLE III
INDUCTANCES OF FUSION TARGET CONCEPTS

Concept	L_o (nH)	ΔL @ Cr (nH)	L_{total} (nH)	I_{peak} at τ_{imp} (MA in ns)
DEH	4.8	13 (20:1)	17.8	10 in 105
ZPDH	2.3	5.1 (7:1)	7.4	26 in 130
MagLIF	4.0	2.8 (10:1)	6.8	22 in 130

and gains on larger pulsed-power systems. Delivering higher energy to fusion targets may provide more robust ignition, provide higher gains, or provide additional margin for non-idealities in igniting systems on future pulsed-power drivers.

The driver coupling efficiency, η_d, is a strong function of both the change in inductance and the total inductance of the load. MagLIF targets are much smaller than both the DEH (Fig. 13) and ZPDH (Fig. 2). Representative current paths are shown in Fig. 13 with the external current return cylinder removed for clarity. Table III provides estimates of the initial and final inductances for the DEH, ZPDH, and MagLIF calculated to various convergence ratios. The measured peak current and time to peak current is also given. High inductance in the DEH configuration resulted in lower peak current coupled from the generator to the wire arrays (10 MA). The ZPDH and MagLIF concepts both have a much higher coupling efficiency from the generator because of the lower inductances involved. Initial MagLIF experiments on Z suggest full delivery of up to 22 MA to the liner, clearly favorable for MagLIF compared to the DEH.

Tables IV–VI summarize results from specific indirect- and direct-drive target point designs developed with 2D-RHD and 2D-RMHD codes [27], [30], [31], [123]. The tables provide the peak current $({\rm I_{peak}})$, the facility energy storage $({\rm E_{store}})$, the energy delivered to the load $({\rm E_{load}})$, the energy in X-rays for indirect drive $({\rm E_{xray}})$, the energy absorbed by the target

TABLE IV
COMPARISON OF INDIRECT DRIVE DEH SCALING

	Z [24-26]	High-Yield [27]	GJ-Yield (IFE) [123]
I_{peak} (MA)	10	2 x 70	2 x 150
E_{store} (MJ)	11.4	380	2500
E_{load} (MJ)	1.1	38	220
E_{xray} (MJ)	0.7	19	110
E_{target} (MJ)	0.015	1.2	8.6
E_{fuel} (MJ)	3e-04	0.18	1
E_{fusion} (MJ)	2e-07	460	4500
Q_{HS}	6.7e-04	2550	4500
Q_E	1.8e-8	1.2	3
η_d (%)	10	10	8.8
η_x (%)	64	50	50
η_c (%)	2.1	6.2	7.8
η_f (%)	2.0	15	12
η_t (%)	0.0026	0.05	0.04

TABLE V
COMPARISON OF DEH ON Z (INDIRECT DRIVE) TO MagLIF ON REFURBISHED Z (DIRECT DRIVE)

	Z (DEH) [24-26]	ZR [30] (Gas MagLIF)	Ratio (MagLIF/DEH)
I_{peak} (MA)	10	26	6.7 (~I^2)
E_{store} (MJ)	11.4	26	2.3
E_{load} (MJ)	1.1	1.9	1.7
E_{xray} (MJ)	0.7	NA	NA
E_{target} (MJ)	0.015	0.7	47
E_{fuel} (MJ)	3e-04	0.1	330
E_{fusion} (MJ)	2e-07	>0.1	5.e5
Q_{HS}	6.7e-04	>1	1500
Q_E	1.8e-8	3.8e-3	2.5e5
η_d (%)	10	7.3	0.7
η_x (%)	64	(100)	1.6
η_c (%)	2.1	37	18
η_f (%)	2.0	14.3	7
η_t (%)	0.0026	0.38	150

(E_{target}), the energy absorbed by the fuel (E_{fuel}), and the predicted fusion yield (E_{fusion}). The tables also list the physics gain of the hot spot ($Q_{HS} = E_{fusion}/E_{fuel}$) and the engineering gain of the facility ($Q_E = E_{fusion}/E_{store}$). The first is relevant for fusion gain physics, the second for the feasibility of the concept for high yield, and for IFE. The efficiencies of the various stages and the total coupling efficiency to the fuel are also provided. Perhaps the most meaningful metric for future applications to generation of high yields as well as IFE is the efficiency of delivery of energy to the fuel (η_t), as well as the overall gain of the facility ($Q_E = E_{fusion}/E_{store}$).

Table IV compares some of these metrics for indirect-drive capsules driven by the DEH concept on Z, the high-yield point design [27], and a DEH point design that might be applied to high yield fusion or IFE [123]. The maximum energy that could be absorbed by the fuel for 3-mm capsules on Z (300 J) and potentially on refurbished Z ($<$ 1 kJ) is not very interesting. Scaling the secondary hohlraum temperature from 70 eV on Z to 220 eV on a 60 MA driver increases both η_c and η_f. The DEH scaling to high yield (~500 MJ at 60 MA) could deliver $8X$ the energy to the capsule, and $10X$ the energy to the fuel as the NIF facility making the capsule implosion more robust. Although designs suggest that the DEH could also scale to GJ yields of interest for IFE, the facility stored energy (~2.5 GJ) and required currents (2×150 MA) are unreasonably large. The overall efficiency ($< 0.1\%$), and engineering Q_E are low.

Table V provides a comparison of the same metrics for the indirect-drive DEH on pre-refurbished Z and the direct-drive gas-filled MagLIF concept on present Z [30]. Direct-drive targets eliminate η_x, and increase η_c and η_f significantly. The MagLIF designs are superior, whether one considers energy delivered, efficiency of total delivery of energy to the fuel, or the potential yield. Such increases in efficiency and potential performance are worth the introduction of new technical risks (such as liner instability) and other potentially unknown risks. The possibility of achieving *scientific breakeven* on Z ($Q_{HS} = 1$, defined as fusion energy out = energy absorbed in the fuel) highlights the significance of direct drive for pulsed power. The fuel pressure at stagnation at which scientific breakeven is predicted to occur is 3 GBars [30]. This is significantly lower than those discussed in Section II that were required for hot spot ignition. The large increase in coupling efficiency and reduction in required fuel pressure is a potential breakthrough worthy of scientific study since it promises to reduce the cost, facility size, and complexity of attaining high fusion yields in the laboratory. It should be noted that ZPDH targets could deliver up to perhaps $>$ 60 kJ to indirect-drive capsules on Z compared to $>$ 700 kJ for MagLIF, hence MagLIF is potentially up to $12X$ more energy rich than the ZPDH as well.

TABLE VI
COMPARISON OF THE DEH AND HIGH GAIN MagLIF FOR GJ-CLASS YIELDS

	GJ-Yield DEH [123]	GJ-Yield MagLIF [31]	Ratio (MagLIF/DEH)
I_{peak} (MA)	2 x 150	70	0.1 (~I^2)
E_{store} (MJ)	2500	200	0.08
E_{load} (MJ)	220	21	0.09
E_{xray} (MJ)	110	NA	NA
E_{target} (MJ)	8.6	9	1
E_{fuel} (MJ)	1	1.2	1.2
E_{fusion} (MJ)	4,500	10,000	2.2
Q_{HS}	4,500	8,330	1.9
Q_E	1.8	50	28
η_d (%)	8.8	10.5	1.2
η_x (%)	50	(100)	2
η_c (%)	7.8	43	5.5
η_f (%)	11.6	13.3	1.15
η_t (%)	0.04	0.6	15

Table VI compares the indirect-drive DEH and direct-drive MagLIF with a cryogenic fuel layer [31] at conditions relevant for national security missions or IFE (GJ-class-yields). Again, direct-drive targets eliminate η_x, and increase η_c and η_f. The predicted fusion yield is increased significantly, and the driver energy required to obtain those yields is decreased significantly. These data show that the MagLIF concept offers considerable potential improvement for fusion systems on Z and is potentially a better path to high-yield fusion. MagLIF offers an increase in facility Q_E of more than $25X$ to 50 total and an increase in efficiency of energy coupled to the fuel of

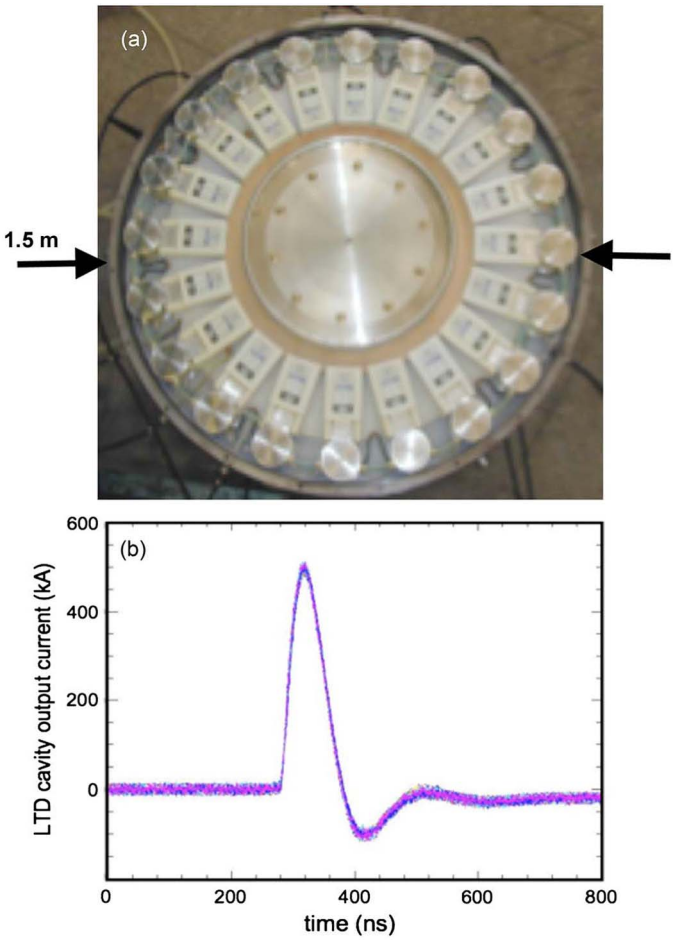

Fig. 14. (a) 50 GW cavity prototype, (b) overlay of 200 consecutive pulses taken at 2/min from [124].

more than a factor of $15X$ to of order 0.6%. This may be of interest for IFE systems.

We note that the driver coupling efficiency, $\eta_{\rm d}$, was constant for all of these indirect and direct-drive targets at about $\eta_{\rm d} \sim 9$ to 11%, with implosion times of order 100 ns. Driver coupling efficiency could be increased up to $\sim 30\%$ if implosion times of $\sim$250 ns could be used. Simulations suggest that optimization of both direct-drive targets (η_c, η_f) and the pulsed-power generators that drive (η_d) them could potentially increase the total fuel coupling efficiency $\eta_{\rm t}$ to 3%.

VI. Driver Designs

In parallel with advances in fusion target designs, the last few years have seen significant progress in efficient, repetitive driver technology [124]–[128]. The linear transformer driver (LTD) is a modular induction cavity that can be configured to produce a high voltage pulse of 70 to 300 ns length, with at least twice the efficiency of the conventional pulsed-power architecture implemented on Z. LTD's have been called "The most significant advance in pulsed power since the invention of the Marx bank in 1924" [129]. Fig. 14(a) shows an early 50 GW prototype cavity developed by Mazarakis *et al.* [124]–[126]. The LTD is a compact induction module consisting of identical capacitor-switch sub-modules or "bricks" connected in parallel to achieve low impedance (high current) [126]. The efficiency of producing a pulse with the desired $\sim$100 ns width is 70%.

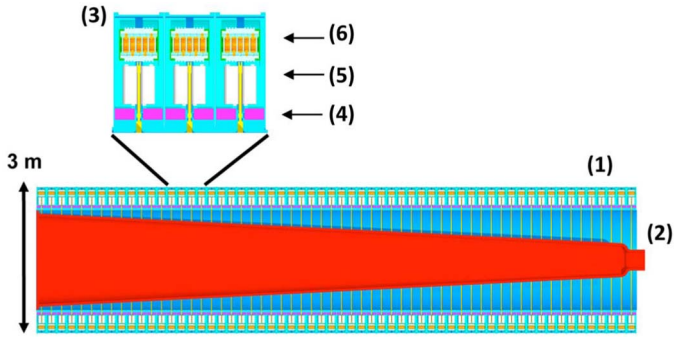

Fig. 15. 60 cavity water line voltage adder module from [128] showing (1) 60 cavity module, (2) tapered central electrode to match module impedance as a function of length, (3) enlarged view of 3 cavities, with (4) magnetic cores, (5) capacitors, and (6) switches.

This can be compared to 35% for the nominal architecture of the standard multi-module facilities such as Z or ZR. The efficiency is higher because the pulse is produced at the desired width, eliminating the need for pulse forming elements in the standard architecture that introduce loss.

Olson and Mazarakis *et al.* adopted vacuum-insulated LTDs as part of a nascent IFE program [130], [131]. The LTD can easily be fired with high repetition rates. Cavity tests at 50 GW have more than 12 000 pulses at 2 per minute, with no failures [125]. LTD cavity components have shown up to 37 000 pulses, also with no failures [126]. Fig. 14(b) shows an overlay of 200 pulses produced by the prototype cavity [125], demonstrating high reproducibility. Ten cavities for a 1 TW LTD module capable of repetition rates of 0.1-Hz have been constructed. Integration tests of these 10 cavities as a water-line adder are planned in the coming years, at full driver power levels for each cavity (100 GW). Recently, further optimization has increased the LTD output current with a fixed LTD cavity size [127].

High voltage is obtained by placing the induction cavities in series. Voltage addition can be done in vacuum along a magnetically insulated transmission line [125] or in water along a water-insulated transmission line [128]. Water is preferred over vacuum since it could provide higher efficiency, longer lifetime, more straightforward integration of hundreds of modules, shielding of the driver modules from neutrons, as well as the ability to more easily shape the current pulse because of a longer transit time between cavities and modules in water [128]. Fig. 15 shows an idealized 6 MV, 1 MA (6 TW) module consisting of 60 identical cavities adding the voltage along a matched impedance water transmission line [128]. These modules consist of a large number of identical capacitors, switches, cores, and other components, and thus the modules are highly amenable to mass production with low per unit cost. Furthermore, the LTD approach uses many low voltage switches (200 kV) rather than a single high voltage 6 MV switch [132]. Stygar *et al.* estimate that the use of many low voltage switches could make the entire system considerably more reliable [53], [54], providing significant benefit to systems with hundreds of modules.

Such modules are combined in a patented, integrated architecture to produce efficient, high current drivers capable of peak currents of 50–100 MA in 120 ns, (within driver diameters of 35–104 m) and delivering up to 20 MJ of magnetic energy to loads [53], [54]. This architecture utilizes several

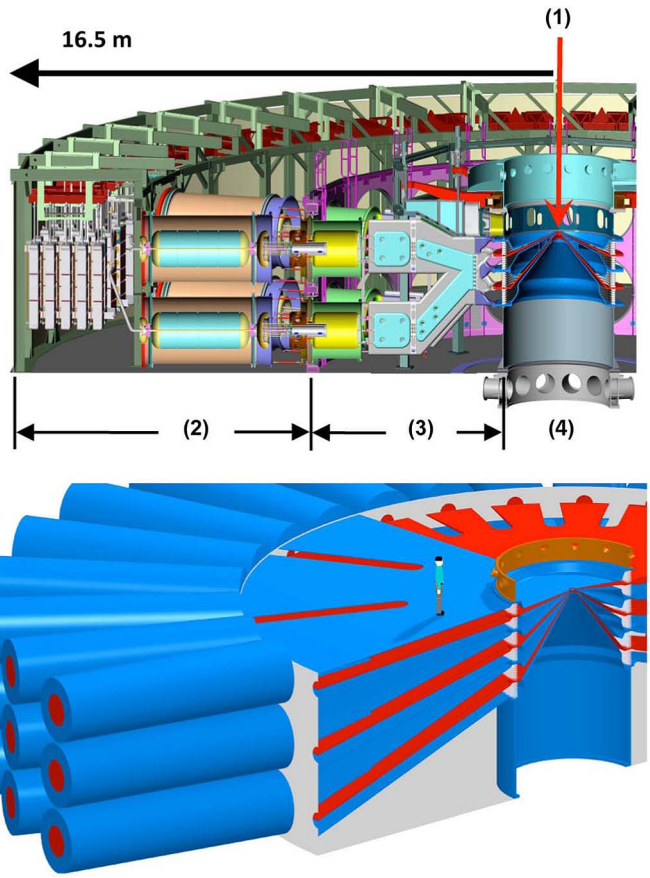

Fig. 16. Comparison of the Z architecture (top) [28], [29] with the new LTD architecture (bottom) [53], [54] with (1) target in central vacuum section, (2) oil section, (3) water section, (4) vacuum section. Various sections of the two machines are approximately aligned. The LTD cavities in section (2) each contain oil, but the modules add voltage in water, as in Fig. 15.

unique elements in combination including LTD modules, and a water-insulated exponential impedance transformer for high efficiency electrical power transport and impedance matching. As an example of the potential of this technology, Fig. 16 compares a cross section of the Z facility with a conceptual design by Stygar based on the LTD architecture [133]. The Z facility is a 26 MA, 22 MJ, 80 TW driver in a 33-m diameter. The conceptual LTD driver would be a 50 MA, 50 MJ, 300 TW driver in a 35-m diameter.

Achieving currents of 60–70 MA required for high gain (G$\sim$100–1000:1) with cryogenic MagLIF [31] would require a facility diameter of 55 m to 85 m [54] and storing energies of 130–200 MJ. Such architectures have been utilized in Tables IV–VI to drive the fusion targets. Prior to this work with LTD drivers and new architectures, there was no integrated pulsed-power generator design that could achieve the electrical powers and currents necessary for high yield fusion. The reproducibility, efficiency, and high reliability of this technology make it attractive for NNSA single-shot applications. The ability to reliably and repetitively pulse the LTD technology makes it attractive for IFE.

VII. Conclusion

The physics basis for the z-pinch indirectly driven capsule designs and the radiation symmetry control are the same as for capsule targets on the NIF. Ignition on the NIF could validate the z-pinch-driven indirect-drive high yield capsule designs. Increased energy delivery to indirect-drive capsules in pulsed-power systems could lower the technical risk for ignition and gain. The primary difference and the chief remaining risks are the issues of z-pinch X-ray power scaling and pulse shaping for both concepts, as well as symmetry control for the ZPDH. It is noteworthy that further progress in integrated designs and scaling for indirect-drive concepts would require increased sophistication in the simulation of MDIs for X-ray source production and many validation experiments. Likewise, progress in direct-drive MDIs for direct-drive fuel compression will also require increasing sophistication in the simulation of z-pinch implosions and validation experiments. Importantly, progress in the understanding and control of z-pinch implosion and stagnation physics in the MagLIF concept could lead directly to significant increases in fusion target performance on *presently available drivers*. Furthermore, given the masses of the z-pinch loads needed for high-yield indirect-drive fusion at currents of 60–70 MA, it is very likely that those loads will also be solid liners rather than wire arrays. In this sense, we are continuing to make progress on both indirect and direct-drive concepts.

There are not many methods to make fusion ignition and high gain easier. The pulsed-power-driven MagLIF concept combines a number of the methods discussed in the literature into one integrated concept, driven by a compact, low-cost, MJ-class, and efficient driver technology. The promise of MagLIF of a more efficient method of assembling, compressing, and igniting fuel is worth the introduction of new technical risks. Simulations indicate that the new target design elements of increased absorbed energy, larger target sizes and fuel volumes, fuel pre-heat, and pre-magnetization, may reduce requirements on fuel ρR for significant yield from 300 $\mathrm{mg/cm^2}$ to 30 $\mathrm{mg/cm^2}$, the requirements on implosion velocity from 35 $\mathrm{cm/\mu s}$ to 10 $\mathrm{cm/\mu s}$, and the requirements for fuel convergence ratio from 35 : 1 to 23 : 1. Furthermore, the large delivered energies to the target ($\sim$500 kJ) means the fusion target implosion experiments can be performed in relevant physics regimes and spatial scales.

There are many issues that need to be studied for MagLIF, including all of the usual issues for ICF [41]–[44], as well as some new ones. While direct-drive targets are compelling from an efficiency point of view, if they do not work because of instabilities, they will ultimately not offer any advantage over indirect drive. The MRT instability and deceleration phase liner-fuel mix at stagnation are believed to be among the largest threats to direct-drive concepts relying on magnetic pressure and magnetized fuel. Encouragingly, our initial experiments suggest that the simulation design tools used to design the MagLIF concept capture the MRT physics well [32]–[35]. The fuel pre-heat conditions are within factors of a few of previously demonstrated gas target experiments [119], which have also been modeled with our design tools. Ultimately, determining the feasibility of this concept will require integrated experiments. The first integrated physics experiments coupling of order 500 kJ to fusion targets are planned to begin in 2013. We have planned five years of validation experiments

to provide an assessment of the potential for this concept (see Table II).

Our eventual goal is a *scaled scientific breakeven*. Scaled breakeven would be a fusion neutron yield with D_2 fuel that would scale to scientific breakeven if DT fuel was used, and also if a peak current of about 27 MA was coupled to the target. This would be a D_2 neutron yield of $\sim$0.5 kJ. Achieving a significant fraction of this yield would represent a high level of target physics understanding with remaining uncertainties. Our first attempts at scaled scientific breakeven meeting all the requirements for the present MagLIF point design (except the use of DT fuel) will occur in 2016 and after. An extensive campaign of integrated implosion experiments and experiments focused on selected physics issues will be carried out over the next five years to validate these simulations and these MDI target design elements.

MagLIF targets may also provide a potential path to multi-GJ-class single-shot yields with cryogenic fuel layers. Such targets may be able to generate high energy density conditions in the laboratory suitable for stockpile stewardship missions. Pulsed-power driver architectures based on LTDs for obtaining these yields are under development for ICF and other missions. LTDs are also rep-rateable and scalable and may therefore also have application to IFE. Application of any target concept to power production for IFE will require the achievement of high *average* fusion thermal power. This will require, among many other things: 1) a low-cost, efficient, rep-rate driver of suitable size, 2) robustly achievable fusion events with sufficient gain and yield, 3) a robust, low-cost method to repetitively couple the driver and target, and 4) the nuclear fusion science of a low-cost, survivable fusion chamber to contain the events, shield the driver, harness the yield to produce heat coupled to a thermodynamic cycle, and provide breeding of tritium fuel.

Previous concepts for IFE based on pulsed-power indirect drive proposed ten fusion chambers and drivers, each operating at repetition frequency of 0.1 Hz, to achieve an effective rep-rate of 1 Hz and a fusion thermal power of $\sim$3 GW_{th} [130], [131]. The driver and target were coupled mechanically with low-cost mechanically rigid recyclable transmission lines (RTLs). Larger yields, possibly provided by direct drive, may permit adequate average fusion thermal power with a single fusion driver and chamber operating at 0.1 Hz [134]. Lower net rep-rates could significantly reduce the cost and complexity of the RTL concept. However, larger yields might ultimately make the driver and chamber too costly. The system and cost optimization among driver size, fusion yields, feasible rep-rate, and fusion chamber is complex and has not been undertaken in a systematic way. Other pulsed-power concepts, employing different drivers, targets, and different methods of driver-target coupling at lower yields and larger rep-rate have also been proposed [83], [135].

Our ICF research program over the next five years will be an evaluation of the key enabling physics of direct-drive fusion implosions with MDIs and an evaluation of some of the key enabling technologies including highly reliable, repetitive LTD's. These are also the first steps that must be taken toward an integrated IFE system.

APPENDIX
LINER IMPLOSION MODEL

Limits on z-pinch implosion velocities can be determined if we consider the equation of motion for the radius, r, of a magnetically driven cylinder:

$$\frac{d^2r}{dt^2} = -\left(\frac{B^2}{2\mu_o}\right)\frac{2\pi rl}{m} = -\left(\frac{\mu_o}{4\pi}\right)\frac{I^2 l}{mr} \tag{A1}$$

where B is the field, l the length, m is mass, and I the current. When this equation is cast in dimensionless form, normalizing variables to mass m_o, length l_o, characteristic current I_p, and time τ, a dimensionless parameter Π emerges [136]:

$$\Pi = \left(\frac{\mu_o}{4\pi}\right)\frac{I_p^2 l_o \tau^2}{m_o r_o^2}. \tag{A2}$$

Implosion characteristics are defined by the choice of Π. Solve (A2) for the characteristic time, τ:

$$\tau = \left(\Pi\frac{4\pi}{\mu_o}\frac{m_o}{l_o}\frac{r_o^2}{I_p^2}\right)^{1/2} = \Pi^{1/2}\tau_A \tag{A3}$$

where τ_A is the characteristic acceleration time for constant current. Π captures the relationship between pinch mass and radius and the peak current of the driver. Thus, Π varies for different pulsed-power generators with different shapes of the current pulse resulting in different acceleration histories. Π also varies for different z-pinch optimization strategies. Π required to maximize the kinetic energy delivered to a z-pinch load will be different than that required to maximize the electrical power delivered to the load.

With a constant current drive, (A1) can be solved analytically. The solution gives an implosion time τ_I of the system (the time at which the pinch reaches the axis) that is defined in terms of the characteristic time τ_A from (A3):

$$\tau_I = \sqrt{\frac{\pi}{2}}\tau_A. \tag{A4}$$

For a constant current system, therefore, $\Pi = \pi/2 = 1.56$.

Constant current drive is unattainable in any inductively coupled implosion system. The next most sophisticated treatment is to assume a linearly rising current waveform $I(t) = (dI/dt) * t$, where dI/dt is the effective rate of rise of the current pulse. A linearly rising current pulse is exact for a constant voltage pulsed-power generator charging a constant inductance transmission line and load:

$$I(t) = \frac{\int V(t)dt}{L} = \frac{V_o}{L}t. \tag{A5}$$

Here, V_o is the amplitude of the rectangular voltage pulse and the dI/dt of the current is given by $dI/dt = V_o/L$. Such a treatment neglects the interaction of the pulsed-power generator circuit with the time-changing inductance of the load. However, dI/dt is the zeroth order, most important characteristic of the generator. This model avoids detailed treatment of the pulsed-power system or current losses in the system. It provides an upper bound on the implosion velocity and lower bound on the implosion time for the z-pinch.

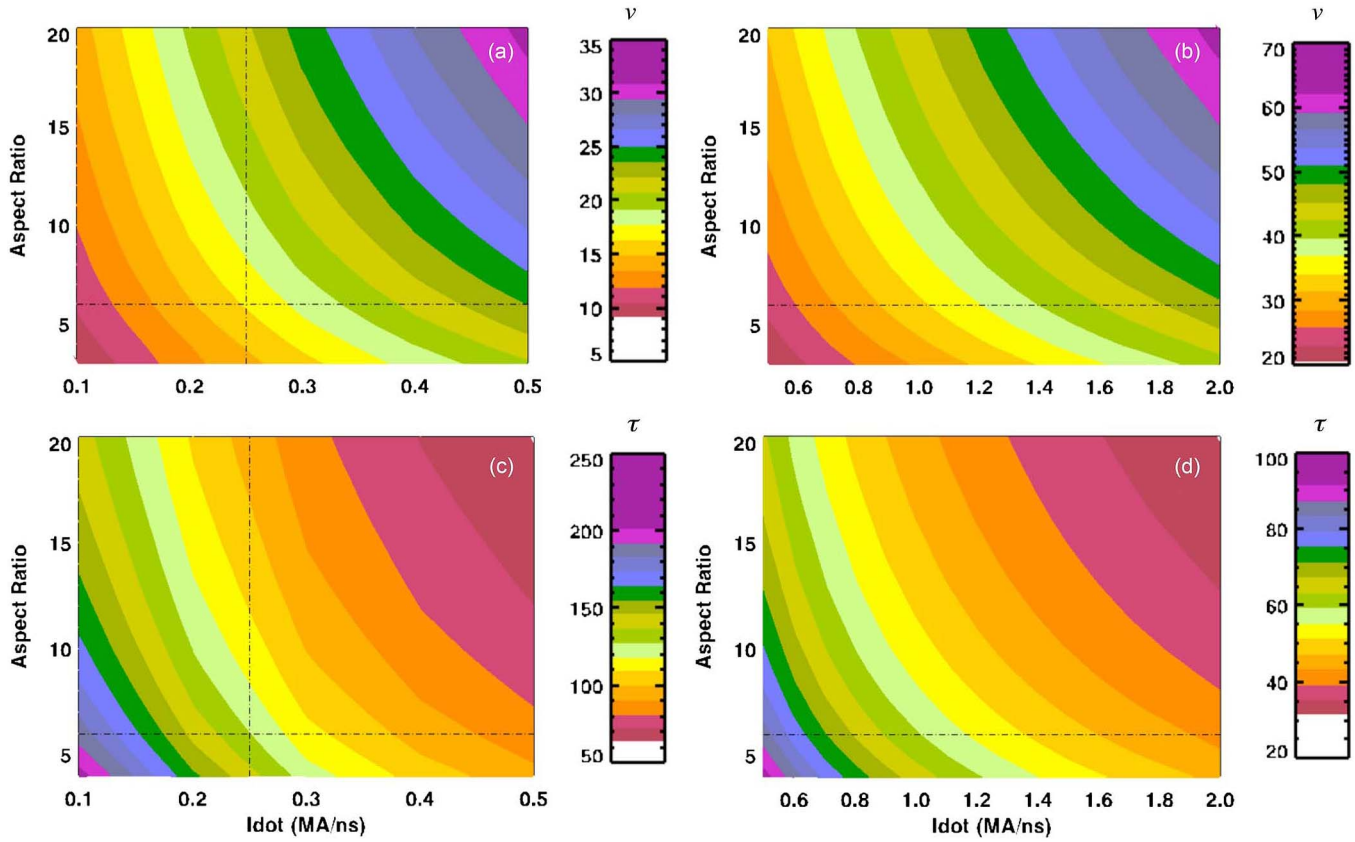

Fig. 17. (a), (b) The implosion velocity v (cm/μs) as a function of aspect ratio (A_R) and dI/dt (MA/ns) for $Cr = 20:1$. The velocity scales as $\sqrt{\ln(Cr)}$ so a change of Cr from 20 : 1 to 10 : 1 only reduces v by 14%. (c), (d) The implosion time τ (ns) as a function of aspect ratio (A_R) and dI/dt for $\mathrm{r_o} = 0.34$ cm. The time scales linearly with $\mathrm{r_o}$. Dotted lines are shown on the plots at $A_R = 6$ and $dI/dt = 0.25$ MA/ns planned for the initial MagLIF experiment [30].

Assume, in (A3) that $I_p = (dI/dt) * \tau$ and solve for τ

$$\tau = \left[\Pi \frac{4\pi}{\mu_o} \frac{m_o}{(dI/dt)^2} \frac{r_o^2}{l_o}\right]^{1/4} \tag{A6}$$

[note the fourth root of this quantity rather than square root in (A3)]. Equation (A1) was solved numerically for a wide range of z-pinch masses, m_o, and dI/dt, discussed below. Using A6 as a scaling relationship, we find that the characteristic implosion time, $\tau_{dI/dt}$, is given by:

$$\tau_{dI/dt} = \left[\Pi \frac{4\pi}{\mu_o} \frac{m_o}{(dI/dt)^2} \frac{r_o^2}{l_o}\right]^{1/4} = \Pi^{1/4} \tau_A' = 1.717 \tau_A'. \tag{A7}$$

Here, τ_A' is the characteristic acceleration time for linearly rising current. The numerical solution shows $\Pi = 8.7$ for constant dI/dt.

For liners, following Slutz *et al.* [30], we have the following for liner mass in terms of ρ_L the liner material density, where $A_R = \mathrm{r_o}/(\mathrm{r_o} - \mathrm{r_i})$ is the liner aspect ratio, with $\mathrm{r_i}$ the inner radius of the liner:

$$m_o = \pi \rho_L l_o \left(r_o^2 - r_i^2\right) = \pi \rho_L l_o r_o^2 \left(\frac{2 - 1/A_R}{A_R}\right). \tag{A8}$$

Substituting (A8) into (A7), we find an expression for the liner implosion time in terms of the liner parameters and the average pulsed-power generator dI/dt:

$$\tau_{dI/dt} = 1.717 \left(\frac{4\pi^2}{\mu_o}\right)^{1/4} \rho_L^{1/4} \left(\frac{r_o^2}{dI/dt}\right)^{1/2} \left(\frac{2 - 1/A_R}{A_R}\right)^{1/4}. \tag{A9}$$

In convenient units:

$$\tau_{dI/dt}[\mathrm{ns}] = 229 \left(dI/dt[\mathrm{MA/ns}]\right)^{-1/2} \left(\rho_L[\mathrm{g/cm^3}]\right)^{1/4} \times r_o[\mathrm{cm}] \left(\frac{2 - 1/A_R}{A_R}\right)^{1/4}. \tag{A10}$$

The analytic solution of (A1) for the implosion velocity for constant current is:

$$v = \left(\frac{\mu_o l_o}{2\pi m_o}\right)^{1/2} I \left[\ln\left(\frac{r_o}{r}\right)\right]^{1/2}. \tag{A11}$$

The numerical solution of (A1) for the case with constant dI/dt was compared with this expression and provides excellent scaling to within 2% over the entire range and $0.1 < \mathrm{r_o} < 1.0$ cm. This scan encompasses a range of $4 \le A_R \le 20$, $0.1 \le dI/dt \le 2$ MA/ns, and $10 \le C_r \le 30$, and corresponds to liner masses of 25 to 170 mg, and liner thicknesses of 125 to 1000 μm

for an $r_o = 0.3$ cm. Fitting the numerical solution to this scaling expression, we find (A12):

$$v_{imp} = 0.9 \left(\frac{\mu_o l_o}{2\pi m_o}\right)^{1/2} \frac{dI}{dt} \tau_{dI/dt} \left[\ln\left(\frac{r_o}{r}\right)\right]^{1/2}. \quad \text{(A12)}$$

The numerical solution is within 10% of the constant current solution because the liner continues to accelerate into the axis with a constant dI/dt. We note that it is the convergence ratio of the current (not the mass) that will be important for determining the implosion velocity. The convergence of the current is smaller than the convergence of the fuel, for thick liners. Substituting in this expression for m_o from (A8) and $\tau_{dI/dt}$ from (A7), we find

$$v_{imp} = 0.9 \left(\frac{3\mu_o^{1/2}}{\pi}\right)^{1/2} (dI/dt)^{1/2} \rho_L^{-1/4} \times \left(\frac{A_R}{2 - 1/A_R}\right)^{1/4} [\ln(Cr)]^{1/2}. \quad \text{(A13)}$$

In convenient units:

$$v_{imp}[\text{cm}/\mu\text{s}] = 16.4 \left(dI/dt[\text{MA/ns}]\right)^{1/2} \left(\rho_L[\text{g/cm}^3]\right)^{-1/4} \times \left(\frac{A_R}{2 - 1/A_R}\right)^{1/4} [ln(Cr)]^{1/2}. \quad \text{(A14)}$$

Plots of (A10) and (A14) are shown in Fig. 17.

ACKNOWLEDGMENT

We wish to thank our colleagues at the Cornell University, Ecole Polytechnique, Imperial College of London, General Atomics, Lawrence Livermore Laboratory, Los Alamos Laboratory, University of Michigan, Naval Research Laboratory, University of Nevada at Reno, NNSA, Princeton University, Voss Scientific, Weizmann Institute, and the University of Wisconsin for many helpful discussions. We thank Brent Blue, Jerry Chittenden, John Giuliani, Jim Hammer, Dave Hanson, Tom Intrator, Chris Keane, Jim Knauer, Keith LeChien, Dillon McDaniel, Aaron Miles, David Montgomery, Craig Olson, John Perkins, Dmitri Ryutov, Pace VanDevender, Sasha Velikovich, and Doug Wilson for valuable suggestions and conversations. We also would like to acknowledge our many retired and former colleagues from the pulsed-power program who helped to lay the foundation for the work we are now doing.

REFERENCES

[1] M. Keith Matzen, M. A. Sweeney, R. G. Adams, J. R. Asay, J. E. Bailey, G. R. Bennett, D. E. Bliss, D. D. Bloomquist, T. A. Brunner, R. B. Campbell, G. A. Chandler, C. A. Coverdale, M. E. Cuneo, J.-P. Davis, C. Deeney, M. P. Desjarlais, G. L. Donovan, C. J. Garasi, T. A. Haill, C. A. Hall, D. L. Hanson, M. J. Hurst, B. Jones, M. D. Knudson, R. J. Leeper, R. W. Lemke, M. G. Mazarakis, D. H. McDaniel, T. A. Mehlhorn, T. J. Nash, C. L. Olson, J. L. Porter, P. K. Rambo, S. E. Rosenthal, G. A. Rochau, L. E. Ruggles, C. L. Ruiz, T. W. L. Sanford, J. F. Seamen, D. B. Sinars, S. A. Slutz, I. C. Smith, K. W. Struve, W. A. Stygar, R. A. Vesey, E. A. Weinbrecht, D. F. Wenger, and E. P. Yu, "Pulsed-power-driven high energy density physics and inertial confinement fusion research," *Phys. Plasmas*, vol. 12, no. 5, p. 055503, May 2005.

[2] M. E. Cuneo, E. M. Waisman, S. V. Lebedev, J. P. Chittenden, W. A. Stygar, G. A. Chandler, R. A. Vesey, E. P. Yu, T. J. Nash, D. E. Bliss, G. S. Sarkisov, T. C. Wagoner, G. R. Bennett, D. B. Sinars, J. L. Porter, W. W. Simpson, L. E. Ruggles, D. F. Wenger, C. J. Garasi, B. V. Oliver, R. A. Aragon, W. E. Fowler, M. C. Hettrick, G. C. Idzorek, D. Johnson, K. Keller, S. E. Lazier, J. S. McGurn, T. A. Mehlhorn, T. Moore, D. S. Nielsen, J. Pyle, S. Speas, K. W. Struve, and J. A. Torres, "Characteristics and scaling of tungsten-wire-array z-pinch implosion dynamics at 20 MA," *Phys. Rev. E, Stat. Nonlin., Soft Matter Phys.*, vol. 71, no. 4, p. 046406, Apr. 2005.

[3] B. Jones, C. A. Coverdale, C. Deeney, D. B. Sinars, E. M. Waisman, M. E. Cuneo, D. J. Ampleford, P. D. LePell, K. R. Cochrane, J. W. Thornhill, J. P. Apruzese, A. Dasgupta, K. G. Whitney, R. W. Clark, and J. P. Chittenden, "Implosion dynamics and K-shell X-ray generation in large diameter stainless steel wire array Z pinches with various nesting configurations," *Phys. Plasmas*, vol. 15, no. 12, p. 122 703, Dec. 2008.

[4] C. Coverdale, B. Jones, D. J. Ampleford, J. Chittenden, C. Jennings, J. W. Thornhill, J. P. Apruzese, R. W. Clark, K. G. Whitney, A. Dasgupta, J. Davis, J. Guiliani, P. D. LePell, C. Deeney, D. B. Sinars, and M. E. Cuneo, "K-shell X-ray sources at the Z accelerator," *High Energy Density Phys.*, vol. 6, no. 2, pp. 143–152, Jun. 2010.

[5] M. D. Knudson, M. P. Desjarlais, R. W. Lemke, T. R. Mattsson, M. French, N. Nettelmann, and R. Redmer, "Probing the interiors of the ice giants: Shock compression of water to 700 GPa and 3.8 g/cm^3," *Phys. Rev. Lett.*, vol. 108, no. 9, p. 091102, Feb. 2012.

[6] S. Root, R. J. Magyar, J. H. Carpenter, D. L. Hanson, and T. R. Mattsson, "Shock compression of a fifth period element: Liquid xenon to 840 GPa," *Phys. Rev. Lett.*, vol. 105, no. 8, p. 085501, Aug. 2010.

[7] C. A. Hall, "Isentropic compression experiments on the Sandia Z accelerator," *Phys. Plasmas*, vol. 7, no. 5, pp. 2069–2075, May 2000.

[8] C. A. Hall, J. R. Asay, M. D. Knudson, W. A. Stygar, R. B. Spielman, T. D. Pointon, D. B. Reisman, A. Toor, and R. C. Cauble, "Experimental configuration for isentropic compression of solids using pulsed magnetic loading," *Rev. Sci. Instrum.*, vol. 72, no. 9, pp. 3587–3595, Sep. 2001.

[9] R. W. Lemke, M. D. Knudson, C. A. Hall, T. A. Haill, P. M. Desjarlais, J. R. Asay, and T. A. Mehlhorn, "Characterization of magnetically accelerated flyer plates," *Phys. Plasmas*, vol. 10, no. 4, pp. 1092–1099, Apr. 2003.

[10] R. W. Lemke, M. D. Knudson, A. C. Robinson, T. A. Haill, K. W. Struve, J. R. Asay, and T. A. Mehlhorn, "Self-consistent, two-dimensional, magnetohydrodynamic simulations of magnetically driven flyer plates," *Phys. Plasmas*, vol. 10, no. 5, pp. 1867–1874, May 2003.

[11] J. P. Davis, C. Deeney, M. D. Knudson, R. W. Lemke, T. D. Pointon, and D. E. Bliss, "Magnetically driven isentropic compression to multimegabar pressures using shaped current pulses on the Z accelerator," *Phys. Plasmas*, vol. 12, no. 5, p. 056310, May 2005.

[12] M. G. Haines, "A review of the dense Z-pinch," *Plasma Phys. Control. Fusion*, vol. 53, no. 9, p. 093001, Sep. 2011.

[13] R. B. Spielman, C. Deeney, G. A. Chandler, M. R. Douglas, D. L. Fehl, M. K. Matzen, D. H. McDaniel, T. J. Nash, J. L. Porter, T. W. L. Sanford, J. F. Seamen, W. A. Stygar, K. W. Struve, S. P. Breeze, J. S. McGurn, J. A. Torres, D. M. Zagar, T. L. Gilliland, D. O. Jobe, J. L. McKenney, R. C. Mock, M. Vargas, and T. Wagoner, "Tungsten wire-array Z-pinch experiments at 200 TW and 2 MJ," *Phys. Plasmas*, vol. 5, no. 5, pp. 2105–2111, May 1998.

[14] V. P. Smirnov, "Fast liners for inertial fusion," *Plasma Phys. Control. Fusion*, vol. 33, no. 13, pp. 1697–1714, Nov. 1991.

[15] J. H. Brownell, R. L. Bowers, K. D. McLenithan, and D. L. Peterson, "Radiation environments produced by plasma z-pinch stagnation on central targets," *Phys. Plasmas*, vol. 5, no. 5, pp. 2071–2080, May 1998.

[16] J. E. Bailey, G. A. Chandler, S. A. Slutz, I. Golovkin, P. W. Lake, J. J. MacFarlane, R. C. Mancini, T. J. Burris-Mog, G. Cooper, R. J. Leeper, T. A. Mehlhorn, T. C. Moore, T. J. Nash, D. S. Nielsen, C. L. Ruiz, D. G. Schroen, and W. A. Varnum, "Hot dense capsule-implosion cores produced by z-pinch dynamic hohlraum radiation," *Phys. Rev. Lett.*, vol. 92, no. 8, p. 085002, Feb. 2004.

[17] C. L. Ruiz, G. W. Cooper, S. A. Slutz, J. E. Bailey, G. A. Chandler, T. J. Nash, T. A. Mehlhorn, R. J. Leeper, D. Fehl, A. J. Nelson, J. Franklin, and L. Ziegler, "Production of thermonuclear neutrons from deuterium-filled capsule implosions driven by z-pinch dynamic hohlraums," *Phys. Rev. Lett.*, vol. 93, no. 1, p. 015001, Jun. 2004.

[18] J. E. Bailey, G. A. Chandler, R. C. Mancini, S. A. Slutz, G. A. Rochau, M. Bump, T. J. Buris-Mog, G. Cooper, G. Dunham, I. Golovkin, J. D. Kilkenny, P. W. Lake, R. J. Leeper, R. Lemke, J. J. MacFarlane, T. A. Mehlhorn, T. C. Moore, T. J. Nash, A. Nikroo, D. S. Nielsen, K. L. Peterson, C. L. Ruiz, D. G. Schroen, D. Steinman, and W. Varnum, "Dynamic hohlraum radiation hydrodynamics," *Phys. Plasmas*, vol. 13, no. 5, p. 056301, May 2006.

[19] S. A. Slutz, K. J. Peterson, R. A. Vesey, R. W. Lemke, J. E. Bailey, W. Varnum, C. L. Ruiz, G. W. Cooper, G. A. Chandler, G. A. Rochau, and T. A. Mehlhorn, "Integrated two-dimensional simulations of dynamic hohlraum driven inertial fusion capsule implosions," *Phys. Plasmas*, vol. 13, no. 10, p. 102 701, Oct. 2006.

[20] G. A. Rochau, J. E. Bailey, G. A. Chandler, G. Cooper, G. S. Dunham, P. Lake, R. J. Leeper, R. W. Lemke, T. A. Mehlhorn, A. Nikroo, K. J. Peterson, C. Ruiz, D. G. Schroen, S. A. Slutz, D. Steinman, W. A. Stygar, and W. Varnum, "High performance capsule implosions driven by the Z-pinch dynamic hohlraum," *Plasma Phys. Control. Fusion*, vol. 49, no. 12B, pp. B591–B600, Dec. 2007.

[21] G. A. Rochau, J. E. Bailey, Y. Maron, G. A. Chandler, G. S. Dunham, D. V. Fisher, V. I. Fisher, R. W. Lemke, J. J. MacFarlane, K. J. Peterson, D. G. Schroen, S. A. Slutz, and E. Stambulchik, "Radiating shock measurements in the Z-pinch dynamic hohlraum," *Phys. Rev. Lett.*, vol. 100, no. 12, p. 125 004, Mar. 2008.

[22] G. A. Rochau, J. E. Bailey, and Y. Maron, "Applied spectroscopy in pulsed power plasmas," *Phys. Plasmas*, vol. 17, no. 5, p. 055501, May 2010.

[23] J. H. Hammer, M. Tabak, S. C. Wilks, J. D. Lindl, D. S. Bailey, P. W. Rambo, A. Toor, G. B. Zimmerman, and J. L. Porter, Jr., "High yield inertial confinement fusion target design for a z-pinch-driven hohlraum," *Phys. Plasmas*, vol. 6, no. 5, pp. 2129–2136, May 1999.

[24] G. R. Bennett, R. A. Vesey, M. E. Cuneo, J. L. Porter, Jr., R. G. Adams, R. A. Aragon, P. K. Rambo, D. C. Rovang, L. E. Ruggles, W. W. Simpson, I. C. Smith, C. S. Speas, K. W. Struve, D. F. Wenger, and O. L. Landen, "Symmetric inertial confinement fusion capsule implosions in a high-yield-scale double-Z-pinch-driven hohlraum on Z," *Phys. Plasmas*, vol. 10, no. 9, pp. 3717–3727, Sep. 2003.

[25] R. A. Vesey, M. E. Cuneo, G. R. Bennett, J. L. Porter, Jr., R. G. Adams, R. A. Aragon, P. K. Rambo, L. E. Ruggles, W. W. Simpson, and I. C. Smith, "Radiation symmetry control for inertial confinement fusion capsule implosions in double Z-pinch hohlraums on Z," *Phys. Plasmas*, vol. 10, no. 5, pp. 1854–1860, May 2003.

[26] M. E. Cuneo, R. A. Vesey, G. R. Bennett, D. B. Sinars, W. A. Stygar, E. M. Waisman, J. L. Porter, P. K. Rambo, I. C. Smith, S. V. Lebedev, J. P. Chittenden, D. E. Bliss, T. J. Nash, G. A. Chandler, B. B. Afeyan, E. P. Yu, R. B. Campbell, R. G. Adams, D. L. Hanson, T. A. Mehlhorn, and M. K. Matzen, "Progress in symmetric ICF capsule implosions and wire-array z-pinch source physics for double-pinch-driven hohlraums," *Plasma Phys. Control. Fusion*, vol. 48, no. 2, pp. R1–R35, Feb. 2006.

[27] R. A. Vesey, M. C. Herrmann, R. W. Lemke, M. P. Desjarlais, M. E. Cuneo, W. A. Stygar, G. R. Bennett, R. B. Campbell, P. J. Christenson, T. A. Mehlhorn, J. L. Porter, and S. A. Slutz, "Target design for high fusion yield with the double Z-pinch-driven hohlraum," *Phys. Plasmas*, vol. 14, no. 5, p. 056302, May 2007.

[28] M. K. Matzen, B. W. Atherton, M. E. Cuneo, G. L. Donovan, C. A. Hall, M. Herrmann, M. L. Kiefer, R. J. Leeper, G. T. Leifeste, F. W. Long, G. R. Mckee, T. A. Mehlhorn, J. L. Porter, L. X. Schneider, K. W. Struve, W. A. Stygar, and E. A. Weinbrecht, "The refurbished Z facility: Capabilities and recent experiments," *Acta Phys. Pol. A*, vol. 115, no. 6, pp. 956–958, Jun. 2009.

[29] D. V. Rose, D. R. Welch, E. A. Madrid, C. L. Miller, R. E. Clark, W. A. Stygar, M. E. Savage, G. A. Rochau, J. E. Bailey, T. J. Nash, M. E. Sceiford, K. W. Struve, P. A. Corcoran, and B. A. Whitney, "Three-dimensional electromagnetic model of the pulsed-power Z-pinch accelerator," *Phys. Rev. ST Accel. Beams*, vol. 13, no. 1, p. 010402, Jan. 2010.

[30] S. A. Slutz, M. C. Herrmann, R. A. Vesey, A. B. Sefkow, D. B. Sinars, D. C. Rovang, K. J. Peterson, and M. E. Cuneo, "Pulsed-power-driven cylindrical liner implosions of laser preheated fuel magnetized with an axial field," *Phys. Plasmas*, vol. 17, no. 5, p. 056303, May 2010.

[31] S. A. Slutz and R. A. Vesey, "High-gain magnetized inertial fusion," *Phys. Rev. Lett.*, vol. 108, no. 2, p. 025003, Jan. 2012.

[32] D. B. Sinars, S. A. Slutz, M. C. Herrmann, R. D. McBride, M. E. Cuneo, K. J. Peterson, R. A. Vesey, C. Nakhleh, B. E. Blue, K. Killebrew, D. Schroen, K. Tomlinson, A. D. Edens, M. R. Lopez, I. C. Smith, J. Shores, V. Bigman, G. R. Bennett, B. W. Atherton, M. Savage, W. A. Stygar, G. T. Leifeste, and J. L. Porter, "Measurements of Magneto-Rayleigh-Taylor instability growth during the implosion of initially solid Al tubes driven by the 20-MA, 100-ns Z facility," *Phys. Rev. Lett.*, vol. 105, no. 18, p. 185 001, Oct. 2010.

[33] D. B. Sinars, S. A. Slutz, M. C. Herrmann, R. D. McBride, M. E. Cuneo, C. A. Jennings, J. P. Chittenden, A. L. Velikovich, K. J. Peterson, R. A. Vesey, C. Nakhleh, E. M. Waisman, B. E. Blue, K. Killebrew, D. Schroen, K. Tomlinson, A. D. Edens, M. R. Lopez, I. C. Smith, J. Shores, V. Bigman, G. R. Bennett, B. W. Atherton, M. Savage, W. A. Stygar, G. T. Leifeste, and J. L. Porter, "Measurements of Magneto-Rayleigh–Taylor instability growth during the implosion of initially solid metal liners," *Phys. Plasmas*, vol. 18, no. 5, p. 056301, May 2011.

[34] D. B. Sinars, K. J. Peterson, S. A. Slutz, M. C. Herrmann, E. P. Yu, M. E. Cuneo, I. C. Smith, G. R. Bennett, B. W. Atherton, J. L. Porter, and D. F. Wenger, "Observation of instability growth in a copper z-pinch target using two-color monochromatic X-ray backlighting," *IEEE Trans. Plasma Sci.*, vol. 39, no. 11, pp. 2408–2409, Nov. 2011.

[35] R. D. McBride, S. A. Slutz, C. A. Jennings, D. B. Sinars, M. E. Cuneo, M. C. Herrmann, R. W. Lemke, M. R. Martin, and B. E. Blue, "Penetrating radiography of imploding and stagnating beryllium liners on the Z accelerator," *Phys. Rev. Lett.*, vol. 109, no. 13, p. 135004, 2012.

[36] D. S. Montgomery, M. Geissel, E. C. Harding, A. B. Sefkow, and D. B. Sinars, "Characterizing MagLIF preheated plasmas using self-Thomson scattering," in *Proc. Amer. Phys. Soc. Div. Plasma Phys.*, vol. TP9, *Bull. Amer. Phys. Soc.*, Salt Lake, UT, 2011, p. 106.

[37] K. J. Peterson, D. B. Sinars, E. P. Yu, M. C. Herrmann, M. E. Cuneo, S. A. Slutz, I. C. Smith, B. W. Atherton, M. D. Knudson, and C. Nakhleh, "Electrothermal instability growth in magnetically driven pulsed power liners," *Phys. Plasmas*, vol. 19, no. 9, p. 092701, Sep. 2012.

[38] R. W. Lemke, M. R. Martin, R. D. McBride, J. P. Davis, M. D. Knudson, D. B. Sinars, I. C. Smith, M. Savage, W. A. Stygar, K. Killebrew, D. G. Flicker, and M. C. Herrmann, "Determination of pressure and density of shocklessly compressed beryllium from X-ray radiography of a magnetically driven cylindrical liner implosion," in *Proc. AIP Conf.*, 2012, vol. 1426, pp. 473–476.

[39] M. R. Martin, R. W. Lemke, R. D. McBride, J.-P. Davis, D. H. Dolan, M. D. Knudson, K. R. Cochrane, D. B. Sinars, I. C. Smith, M. Savage, W. A. Stygar, K. Killebrew, D. G. Flicker, and M. C. Herrmann, "Solid liner implosions on z for producing multi-megabar, shockless, compressions," *Phys. Plasmas*, vol. 19, no. 5, p. 056310, May 2012.

[40] R. W. Lemke and R. D. McBride, private communication, 2012.

[41] J. D. Lindl, "Development of the indirect-drive approach to inertial confinement fusion and the target physics basis for ignition and gain," *Phys. Plasmas*, vol. 2, no. 11, pp. 3933–4025, Nov. 1995.

[42] M. Rosen, "The physics issues that determine inertial confinement fusion target gain and driver requirements," *Phys. Plasmas*, vol. 6, no. 5, pp. 1690–1699, May 1999.

[43] J. D. Lindl, P. Amendt, R. L. Berger, S. G. Glendinning, S. H. Glenzer, S. W. Haan, R. L. Kauffman, O. L. Landen, and L. J. Suter, "The physics basis for ignition using indirect-drive targets on the national ignition facility," *Phys. Plasmas*, vol. 11, no. 2, pp. 339–492, Feb. 2004.

[44] S. Atzeni and J. Meyer-Ter-Vehn, *The Physics of Inertial Fusion*. Oxford, U.K.: Clarendon, 2004.

[45] E. I. Moses, "The national ignition facility and the national ignition campaign," *IEEE Trans. Plasma Sci.*, vol. 38, no. 4, pp. 684–689, Apr. 2010.

[46] J. H. Nuckolls, "Grand challenges of inertial fusion energy," *J. Phys., Conf. Ser.*, vol. 244, no. 1, p. 012007, 2010.

[47] I. R. Lindemuth and R. C. Kirkpatrick, "Parameter space for magnetized fuel targets in inertial confinement fusion," *Nucl. Fusion*, vol. 23, no. 3, pp. 263–284, Mar. 1983.

[48] M. M. Basko, A. J. Kemp, and J. Meyer-ter-Vehn, "Ignition conditions for magnetized target fusion in cylindrical geometry," *Nucl. Fusion*, vol. 40, no. 1, pp. 59–68, Jan. 2000.

[49] T. W. L. Sanford, G. O. Allshouse, B. M. Marder, T. J. Nash, R. C. Mock, R. B. Spielman, J. F. Seamen, J. S. McGurn, D. Jobe, T. L. Gilliland, M. Vargas, K. W. Struve, W. A. Stygar, M. R. Douglas, M. K. Matzen, J. H. Hammer, J. S. De Groot, J. L. Eddleman, D. L. Peterson, D. Mosher, K. G. Whitney, J. W. Thornhill, P. E. Pulsifer, J. P. Apruzese, and Y. Maron, "Improved symmetry greatly increases X-ray power from wire-array Z-pinches," *Phys. Rev. Lett.*, vol. 77, no. 25, pp. 5063–5066, Dec. 1996.

[50] C. Deeney, T. J. Nash, R. B. Spielman, J. F. Seaman, G. C. Chandler, K. W. Struve, J. L. Porter, W. A. Stygar, J. S. McGurn, D. O. Jobe, T. L. Gilliland, J. A. Torres, M. F. Vargas, L. E. Ruggles, S. Breeze, R. C. Mock, M. R. Douglas, D. L. Fehl, D. H. McDaniel, M. K. Matzen, D. L. Peterson, W. Matuska, N. F. Roderick, and J. J. MacFarlane, "Power enhancement by increasing the initial array radius and wire number of tungsten Z pinches," *Phys. Rev. E, Stat., Nonlin., Soft Matter Phys.*, vol. 56, no. 5, pp. 5945–5958, Nov. 1997.

[51] J. E. Bailey, private communication, 2012.

[52] R. A. Vesey, S. A. Slutz, M. C. Herrmann, T. A. Mehlhorn, and R. B. Campbell, "Mode-selective symmetry control for indirect-drive

inertial confinement fusion hohlraums," *Phys. Plasmas*, vol. 15, no. 4, p. 042704, Apr. 2008.

[53] W. A. Stygar, M. E. Cuneo, D. I. Headley, H. C. Ives, R. J. Leeper, M. G. Mazarakis, C. L. Olson, J. L. Porter, T. C. Wagoner, and J. R. Woodworth, "Architecture of petawatt-class z-pinch accelerators," *Phys. Rev. ST Accel. Beams*, vol. 10, no. 3, p. 030401, Mar. 2007.

[54] W. A. Stygar, M. E. Cuneo, D. I. Headley, H. C. Ives, B. Cottrell Ives, J. Ramon, M. G. Leeper, C. L. Mazarakis, J. L. Olson, and T. C. Porter, "Petawatt pulsed-power accelerator," U.S. Patent 7 679 297 B1, Mar. 16, 2010.

[55] S. N. Bland, S. V. Lebedev, J. P. Chittenden, C. Jennings, and M. G. Haines, "Nested wire array Z-pinch experiments operating in the current transfer mode," *Phys. Plasmas*, vol. 10, no. 4, pp. 1100–1112, Apr. 2003.

[56] M. E. Cuneo, R. A. Vesey, D. B. Sinars, J. P. Chittenden, E. M. Waisman, R. W. Lemke, S. V. Lebedev, D. E. Bliss, W. A. Stygar, J. L. Porter, D. G. Schroen, M. G. Mazarakis, G. A. Chandler, and T. A. Mehlhorn, "Demonstration of radiation pulse shaping with nested-tungsten-wire-array Z pinches for high-yield inertial confinement fusion," *Phys. Rev. Lett.*, vol. 95, no. 18, p. 185 001, Oct. 2005.

[57] M. E. Cuneo, D. B. Sinars, E. M. Waisman, D. E. Bliss, W. A. Stygar, R. A. Vesey, R. W. Lemke, I. C. Smith, P. K. Rambo, J. L. Porter, G. A. Chandler, T. J. Nash, M. G. Mazarakis, R. G. Adams, E. P. Yu, K. W. Struve, and T. A. Mehlhorn, "Compact single and nested tungsten-wire-array dynamics at 14–19 MA and applications to inertial confinement fusion," *Phys. Plasmas*, vol. 13, no. 5, p. 056318, May 2006.

[58] R. W. Lemke, R. A. Vesey, M. E. Cuneo, M. P. Desjarlais, and T. A. Mehlhorn, "Z-Pinch requirements for achieving high yield fusion via a z-pinch driven, double ended hohlraum concept," in *Proc. IEEE Int. Conf. Megagauss Magn. Fields High Energy Liner Technol.*, 2007, pp. 507–512.

[59] D. J. Ampleford, S. N. Bland, M. E. Cuneo, S. V. Lebedev, D. B. Sinars, C. A. Jennings, E. M. Waisman, R. A. Vesey, G. N. Hall, F. Suzuki-Vidal, J. P. Chittenden, and S. C. Bott, *Demonstration of radiation pulse shaping capabilities using nested conical wire array Z-pinches*, 2012, to be published.

[60] W. A. Stygar, M. E. Cuneo, R. A. Vesey, H. C. Ives, M. G. Mazarakis, G. A. Chandler, D. L. Fehl, R. J. Leeper, M. K. Matzen, D. H. McDaniel, J. S. McGurn, J. L. McKenney, D. J. Muron, C. L. Olson, J. L. Porter, J. J. Ramirez, J. F. Seamen, C. S. Speas, R. B. Spielman, K. W. Struve, J. A. Torres, E. M. Waisman, T. C. Wagoner, and T. L. Gilliland, "Theoretical z-pinch scaling relations for thermonuclear-fusion experiments," *Phys. Rev. E, Stat. Nonlin., Soft Matter Phys.*, vol. 72, no. 2, p. 026404, Aug. 2005.

[61] W. A. Stygar, H. C. Ives, D. L. Fehl, M. E. Cuneo, M. G. Mazarakis, J. E. Bailey, G. R. Bennett, D. E. Bliss, G. A. Chandler, R. J. Leeper, M. K. Matzen, D. H. McDaniel, J. S. McGurn, J. L. McKenney, L. P. Mix, D. J. Muron, J. L. Porter, J. J. Ramirez, L. E. Ruggles, J. F. Seamen, W. W. Simpson, C. S. Speas, R. B. Spielman, K. W. Struve, J. A. Torres, and R. A. Vesey, "X-ray emission from z pinches at 10^7 A: Current scaling, gap closure, and shot-to-shot fluctuations," *Phys. Rev. E, Stat. Nonlin., Soft Matter Phys.*, vol. 69, no. 4, p. 046403, Apr. 2004.

[62] M. G. Mazarakis, M. E. Cuneo, W. A. Stygar, H. C. Harjes, D. B. Sinars, B. M. Jones, C. Deeney, E. M. Waisman, T. J. Nash, K. W. Struve, and D. H. McDaniel, "X-ray emission current scaling experiments for compact single-tungsten-wire arrays at 80-nanosecond implosion times," *Phys. Rev. E, Stat. Nonlin., Soft Matter Phys.*, vol. 79, no. 1, p. 016412, Jan. 2009.

[63] C. A. Jennings, M. E. Cuneo, E. M. Waisman, D. B. Sinars, D. J. Ampleford, G. R. Bennett, W. A. Stygar, and J. P. Chittenden, "Simulations of the implosion and stagnation of compact wire arrays," *Phys. Plasmas*, vol. 17, no. 9, p. 092703, Sep. 2010.

[64] J. P. Chittenden and C. Jennings, "Development of instabilities in wire arrays," *Phys. Rev. Lett.*, vol. 101, no. 5, p. 055005, Aug. 2008.

[65] E. P. Yu, M. E. Cuneo, M. P. Desjarlais, R. W. Lemke, D. B. Sinars, T. A. Haill, E. M. Waisman, G. R. Bennett, C. A. Jennings, T. A. Mehlhorn, T. A. Brunner, H. L. Hanshaw, J. L. Porter, W. A. Stygar, and L. I. Rudakov, "Three-dimensional effects in trailing mass in the wire-array Z pinch," *Phys. Plasmas*, vol. 15, no. 5, p. 056301, May 2008.

[66] R. W. Lemke, D. B. Sinars, E. M. Waisman, M. E. Cuneo, E. P. Yu, T. A. Haill, H. L. Hanshaw, T. A. Brunner, C. A. Jennings, W. A. Stygar, M. P. Desjarlais, T. A. Mehlhorn, and J. L. Porter, "Effects of mass ablation on the scaling of X-ray power with current in wire-array Z pinches," *Phys. Rev. Lett.*, vol. 102, no. 2, p. 025005, Jan. 2009.

[67] C. A. Jennings, J. P. Chittenden, M. E. Cuneo, W. A. Stygar, D. J. Ampleford, E. M. Waisman, M. Jones, M. E. Savage, K. R. LeChien, and T. C. Wagoner, "Circuit model for driving three dimensional resistive MHD wire array z pinch calculations," *IEEE Trans. Plasma Sci.*, vol. 38, no. 4, pp. 529–539, Apr. 2010.

[68] C. A. Jennings, M. E. Cuneo, D. J. Ampleford, R. Lemke, and J. P. Chittenden, private communication, 2009.

[69] V. L. Kantsyrev, A. S. Safronova, A. A. Esaulov, K. M. Williamson, I. Shrestha, F. Yilmaz, G. C. Osborne, M. E. Weller, N. D. Ouart, V. V. Shlyaptseva, L. I. Rudakov, A. S. Chuvatin, and A. L. Velikovich, "A review of new wire arrays with open and closed magnetic configurations at the 1.6 MA Zebra generator for radiative properties and opacity effects," *High Energy Density Phys.*, vol. 5, no. 3, pp. 115–123, Sep. 2009.

[70] G. N. Hall, J. P. Chittenden, S. N. Bland, S. V. Lebedev, S. C. Bott, C. Jennings, J. B. A. Palmer, and F. Suzuki-Vidal, "Modifying wire-array z-pinch ablation structure using coiled arrays," *Phys. Rev. Lett.*, vol. 100, no. 6, p. 065003, Feb. 2008.

[71] G. N. Hall, S. N. Bland, S. V. Lebedev, J. P. Chittenden, J. Palmer, F. A. Suzuki-Vidal, and S. C. Bott, "Modifying wire-array Z-pinch ablation structure and implosion dynamics using coiled arrays," *IEEE Trans. Plasma Sci.*, vol. 37, no. 4, pp. 520–529, Apr. 2009.

[72] V. V. Ivanov, A. L. Astanovitskiy, D. Papp, J. P. Chittenden, S. N. Bland, and B. Jones, "Study of transparent and nontransparent regimes of implosion in star wire arrays," *Phys. Plasmas*, vol. 17, no. 10, p. 102 702, Oct. 2010.

[73] B. Jones, D. J. Ampleford, R. A. Vesey, M. E. Cuneo, C. A. Coverdale, E. M. Waisman, M. C. Jones, W. E. Fowler, W. A. Stygar, J. D. Serrano, M. P. Vigil, A. A. Esaulov, V. L. Kantsyrev, A. S. Safronova, K. M. Williamson, A. S. Chuvatin, and L. I. Rudakov, "Planar wire-array Z-pinch implosion dynamics and X-ray scaling at multiple-MA drive currents for a compact multisource hohlraum configuration," *Phys. Rev. Lett.*, vol. 104, no. 12, p. 125 001, Mar. 2010.

[74] D. J. Ampleford, C. A. Jennings, S. N. Bland, S. V. Lebedev, J. P. Chittenden, G. N. Hall, F. Suzuki-Vidal, M. E. Cuneo, T. J. Rogers, M. Cleveland, R. D. McBride, J. D. Serrano, B. Peyton, C. A. Coverdale, M. C. Jones, and B. M. Jones, "Investigation of radial wire arrays for inertial confinement fusion and radiation effects science," Sandia Nat. Lab., Albuquerque, NM, Tech. Rep. SAND2010-0833, 2010.

[75] G. A. Rochau, private communication, 2007.

[76] J. S. Lash, G. A. Chandler, G. Cooper, M. Derzon, M. R. Douglas, D. Hebron, R. Leeper, M. K. Matzen, T. A. Mehlhorn, T. Nash, R. Olson, C. Ruiz, T. Sanford, S. A. Slutz, D. L. Peterson, and R. Chrien, "The prospects for high yield ICF with a Z-pinch driven dynamic hohlraum," *Comptes Rendus Acad. Sci.-Ser. IV-Phys.*, vol. 1, no. 6, pp. 759–765, Aug. 2000.

[77] T. A. Mehlhorn, J. E. Bailey, G. Bennett, G. A. Chandler, G. Cooper, M. E. Cuneo, I. Golovkin, D. L. Hanson, R. J. Leeper, J. J. MacFarlane, R. C. Mancini, M. K. Matzen, T. J. Nash, C. L. Olson, J. L. Porter, C. L. Ruiz, D. G. Schroen, S. A. Slutz, W. Varnum, and R. A. Vesey, "Recent experimental results on ICF target implosions by Z-pinch radiation sources and their relevance to ICF ignition studies," *Plasma Phys. Control. Fusion*, vol. 45, no. 12A, pp. A325–A334, Dec. 2003.

[78] G. A. Chandler, D. B. Sinars, K. Peterson, D. E. Bliss, J. E. Bailey, G. Cooper, G. Dunham, R. W. Lemke, G. A. Rochau, C. L. Ruiz, S. A. Slutz, W. S. Varnum, R. J. Leeper, T. A. Mehlhorn, D. G. Schroen, and D. A. Steinman, "Monochromatic backlighting imaging of dynamic hohlraum driven capsule experiments," Sandia Nat. Lab., Albuquerque, NM, Tech. Rep. SAND2005-4533A, 2005.

[79] D. B. Sinars, G. R. Bennett, D. F. Wenger, M. E. Cuneo, D. L. Hanson, J. L. Porter, R. G. Adams, P. K. Rambo, D. C. Rovang, and I. C. Smith, "Monochromatic x-rya imaging experiments on the Sandia National Laboratories Z facility (invited)," *Rev. Sci. Instrum.*, vol. 75, no. 10, pp. 3672–3677, Oct. 2004.

[80] S. A. Slutz, R. A. Vesey, and M. C. Herrmann, "Compensation for time-depenent radiation-drive asymmetries in inertial-fusion capsules," *Phys. Rev. Lett.*, vol. 99, no. 10, p. 175 001, Oct. 2007.

[81] M. C. Herrmann, M. Tabak, and J. D. Lindl, "A generalized scaling law for the ignition energy of inertial confinement fusion capsules," *Nuclear Fusion*, vol. 41, p. 99, Jan. 2001.

[82] D. V. Rose, D. R. Welch, T. P. Hughes, R. E. Clark, and W. A. Stygar, "Plasma evolution and dynamics in high-power vacuum-transmission-line post-hole convolutes," *Phys. Rev. ST Accel. Beams*, vol. 11, no. 6, p. 060401, Jun. 2008.

[83] J. P. VanDevender, M. E. Cuneo, S. A. Slutz, M. Herrmann, R. A. Vesey, D. B. Sinars, D. B. Seidel, L. X. Schneider, K. A. Mikkelson,

V. J. Harper-Slaboszewicz, B. P. Peyton, A. B. Sefkow, and M. K. Matzen, "Plasma power station with quasi spherical direct drive capsule for fusion yield and inverse diode for driver-target coupling," *Fusion Sci. Technol.*, vol. 61, no. 1T, pp. 101–106, Jan. 2012.

[84] J. P. VanDevender, W. L. Langston, M. F. Pasik, R. S. Coats, T. D. Pointon, D. B. Seidel, G. R. McKee, and L. X. Schneider, "New self-magnetically insulated connection of multi-level accelerators to a common load," in *Proc. IEEE Pulsed Power Conf.*, Chicago, IL, Jun. 19–23, 2011, pp. 1003–1008.

[85] J. P. VanDevender, D. B. Seidel, K. A. Mikkelson, R. D. Thomas, V. J. Harper-Slaboszewicz, and B. P. Peyton, "Inverse diode for combination of multiple modules and fusion driver-target standoff," in *Proc. IEEE 18th Pulsed Power Conference*, Chicago, IL, Jun. 19–23, 2011, pp. 1003–1008.

[86] A. J. Harvey-Thompson, S. V. Lebedev, G. Burdiak, E. M. Waisman, G. N. Hall, F. Suzuki-Vidal, S. N. Bland, J. P. Chittenden, P. De Grouchy, E. Khoory, L. Pickworth, J. Skidmore, and G. Swadling, "Suppression of the ablation phase in wire array pinches using a tailored current prepulse," *Phys. Rev. Lett.*, vol. 106, no. 20, p. 205 002, May 2011.

[87] R. C. Kirkpatrick, I. R. Lindemuth, and M. S. Ward, "Magnetized target fusion: An overview," *Fusion Technol.*, vol. 27, no. 3, pp. 201–214, May 1995.

[88] R. P. Drake, J. H. Hammer, C. W. Hartman, L. J. Perkins, and D. D. Ryutov, "Submegajoule liner implosion of a closed field line configuration," *Fusion Technol.*, vol. 30, no. 1, pp. 310–325, Dec. 1996.

[89] R. E. Siemon, I. R. Lindemuth, and K. F. Schoenberg, "Why magnetized target fusion offers a low-cost development path for fusion energy," *Comments Plasma Phys. Control. Fusion*, vol. 18, no. 6, pp. 363–386, 1999.

[90] D. D. Ryutov and R. E. Siemon, "Magnetized plasma configurations for fast liner implosions: A variety of possibilities," *Comments Modern Phys.*, vol. 2, no. 5, pp. C185–C201, 2001.

[91] T. Intrator, M. Taccetti, D. A. Clark, J. H. Degnan, D. Gale, S. Coffey, J. Garcia, P. Rodriguez, W. Sommars, B. Marshall, F. Wysocki, R. Siemon, R. Faehl, K. Forman, R. Bartlett, T. Cavazos, R. J. Faehl, K. Forman, M. H. Frese, D. Fulton, J. C. Gueits, T. W. Hussey, R. Kirkpatrick, G. F. Kiuttu, F. M. Lehr, J. D. Letterio, I. Lindemuth, W. McCullough, R. Moses, R. E. Peterkin, R. E. Reinovsky, N. F. Roderick, E. L. Ruden, K. F. Schoenberg, D. Scudder, J. Shlachter, and G. A. Wurden, "Experimental measurements of a converging flux conserver suitable for compressing a field reversed configuration for magnetized target fusion," *Nucl. Fusion*, vol. 42, no. 2, pp. 211–222, Feb. 2002.

[92] I. R. Lindemuth and R. E. Siemon, "The fundamental parameter space of controlled thermonuclear fusion," *Amer. J. Phys.*, vol. 77, no. 5, pp. 407–416, May 2009.

[93] S. F. Garanin, "The MAGO system (magnetic compression)," *IEEE Trans. Plasma Sci.*, vol. 26, no. 4, pp. 1230–1238, Aug. 1998.

[94] S. F. Garanin, V. I. Mamyshev, and V. B. Yakubov, "The MAGO system: Current status," *IEEE Trans. Plasma Sci.*, vol. 34, no. 5, pp. 2273–2278, Oct. 2006.

[95] G. A. Wurden, T. P. Intrator, and P. E. Sieck, "FRCHX magnetized target fusion HEDLP experiments," presented at the Proc. IAEA Fusion Energy Conf., Geneva, Switzerland, 2008, Paper IC/P4-13. [Online]. Available: http://www-pub.iaea.org/MTCD/Meetings/fec2008pp.asp

[96] Magnetized Target Fusion. [Online]. Available: http://en.wikipedia.org/wiki/Magnetized_target_fusion

[97] E. Fermi, "Super lecture no. 5—Thermal conduction as affected by a magnetic field," Los Alamos Lab., Los Alamos, NM, Los Alamos Lab. Rep. 344, 1945.

[98] R. Landshoff, "Transport phenomenon in a completely ionized gas in presence of a magnetic field," *Phys. Rev.*, vol. 76, no. 7, pp. 904–909, Oct. 1949.

[99] M. M. Widner, C. J. Chang, A. V. Farnsworth, R. J. Leeper, T. S. Prevender, L. Baker, and J. N. Olson, "Neutron production from relativistic electron beam targets," *Bull. Amer. Phys. Soc.*, vol. 22, p. 1139, 1977.

[100] O. V. Gotchev, N. W. Jang, J. P. Knauer, M. D. Barbero, R. Betti, C. K. Li, and R. D. Petrasso, "Magneto-inertial approach to direct-drive laser fusion," *J. Fusion Energy*, vol. 27, no. 1/2, pp. 25–31, Jun. 2008.

[101] O. V. Gotchev, P. Y. Chang, J. P. Knauer, D. D. Meyerhofer, O. Polomarov, J. Frenje, C. K. Li, M. J.-E. Manuel, R. D. Petrasso, J. R. Rygg, F. H. Seguin, and R. Betti, "Laser-driven magnetic-flux compression in high-energy-density plasmas," *Phys. Rev. Lett.*, vol. 103, no. 21, p. 215 004, Nov. 2009.

[102] J. P. Knauer, O. V. Gotchev, P. Y. Chang, D. D. Meyerhofer, O. Polomarov, R. Betti, J. A. Frenje, C. K. Li, M. J.-E. Manuel, R. D. Petrasso, J. R. Rygg, and F. H. Seguin, "Compressing magnetic fields with high-energy lasers," *Phys. Plasmas*, vol. 17, no. 5, p. 056318, May 2010.

[103] P. Y. Chang, G. Fiksel, M. Hohenberger, J. P. Knauer, R. Betti, F. J. Marshall, D. D. Meyerhofer, F. H. Seguin, and R. D. Petrasso, "Fusion yield enhancement in magnetized laser-driven implosions," *Phys. Rev. Lett.*, vol. 107, no. 3, p. 035006, Jul. 2011.

[104] W. M. Parsons, E. O. Ballard, R. R. Bartsch, J. F. Benage, G. A. Bennett, R. L. Bowers, D. W. Bowman, J. H. Brownell, J. C. Cochrane, H. A. Davis, C. A. Ekdahl, R. F. Gribble, J. R. Griego, P. D. Goldstone, M. E. Jones, W. B. Hinckley, K. W. Hosack, R. J. Kasik, H. Lee, E. A. Lopez, I. R. Lindemuth, M. D. Monroe, R. W. Moses, Jr., S. A. Ney, D. Platts, W. A. Reass, H. R. Salazar, G. M. Sandoval, D. W. Scudder, J. S. Shlachter, M. C. Thompson, R. J. Trainor, G. A. Valdez, R. G. Watt, G. A. Wurden, and S. M. Younger, "The Atlas project—A new pulsed power facility for high energy density physics experiments," *IEEE Trans. Plasma Sci.*, vol. 25, no. 2, pp. 205–211, Apr. 1997.

[105] W. L. Baker, M. C. Clark, J. H. Degnan, G. F. Kiuttu, C. R. McClenahan, and R. E. Reinovsky, "Electromagnetic implosion generation of pulsed high-energy-density plasma," *J. Appl. Phys.*, vol. 49, no. 9, pp. 4694–4706, Sep. 1978.

[106] T. J. Nash, D. H. McDaniel, R. J. Leeper, C. D. Deeney, T. W. L. Sanford, K. Struve, and J. S. DeGroot, "Design, simulation, and application of quasi-spherical 100 ns z-pinch implosions driven by tens of megaamperes," *Phys. Plasmas*, vol. 12, no. 5, p. 052705, May 2005.

[107] J. H. Degnan, M. L. Alme, B. S. Austin, J. D. Beason, S. K. Coffey, D. G. Gale, J. D. Graham, J. J. Havranek, T. W. Hussey, G. F. Kiuttu, B. B. Kreh, F. M. Lehr, R. A. Lewis, D. E. Lileikis, D. Morgan, C. A. Outten, R. E. Peterkin, Jr., D. Platts, N. F. Roderick, E. L. Ruden, U. Shumlak, G. A. Smith, W. Sommars, and P. J. Turchi, "Compression of plasma to megabar range using imploding liner," *Phys. Rev. Lett.*, vol. 82, no. 13, pp. 2681–2684, Mar. 1999.

[108] P. K. Rambo, I. C. Smith, J. L. Porter, Jr., M. J. Hurst, C. S. Speas, R. G. Adams, A. J. Garcia, E. Dawson, B. D. Thurston, C. Wakefield, J. W. Kellogg, M. J. Slattery, H. C. Ives, III, R. S. Broyles, J. A. Caird, A. C. Erlandson, J. E. Murray, W. C. Behrendt, N. D. Neilsen, and J. M. Narduzzi, "Z-Beamlet: A multikilojoule, terawatt-class laser system," *Appl. Opt.*, vol. 44, no. 12, pp. 2421–2430, Apr. 2005.

[109] T. J. Awe, B. S. Bauer, S. Fuelling, and R. E. Siemon, "Threshold for thermal ionization of an aluminum surface by pulsed megagauss magnetic field," *Phys. Rev. Lett.*, vol. 104, no. 3, p. 035001, Jan. 2010.

[110] T. J. Awe, B. S. Bauer, S. Fuelling, and R. E. Siemon, "Mitigation of nonthermal plasma production to measure the pulsed magnetic field threshold for the thermal formation of plasma from thick aluminum surface," *Phys. Plasmas*, vol. 18, no. 5, p. 056304, May 2011.

[111] I. R. Lindemuth, R. E. Siemon, B. S. Bauer, M. A. Angelova, and W. L. Atchison, "Computational interpretation of megagauss-magnetic-field-induced metallic surface plasma initiation and evolution," *Phys. Rev. Lett.*, vol. 105, no. 19, p. 195 004, Nov. 2010.

[112] I. C. Blesener, K. S. Blesener, J. B. Greenly, D. A. Hammer, B. R. Kusse, C. E. Seyler, and B. Blue, "Ablation dynamics, precursor formation, and instability studies on thin foil copper liners," in *Proc. IEEE Int. Conf. Plasma Sci.*, Chicago, IL, Jun. 26–30, 2011, p. 1.

[113] D. D. Ryutov, "Selected physics issues of magnetized plasmas," Livermore Nat. Lab., Livermore, CA, Tech. Rep. LLNL-TR-460213, 2010.

[114] Y. Y. Lau, J. C. Zier, I. M. Rittersdorf, M. R. Weis, and R. M. Gilgenbach, "Anisotropy and feedthrough in magneto-Rayleigh-Taylor instability," *Phys. Rev. E, Stat., Nonlin., Soft Matter Phys.*, vol. 83, no. 6, p. 066405, Jun. 2011.

[115] P. Zhang, Y. Y. Lau, I. M. Rittersdorf, M. R. Weis, R. M. Gilgenbach, D. Chalenski, and S. A. Slutz, "Effects of magnetic shear on magneto-Rayleigh-Taylor instability," *Phys. Plasmas*, vol. 19, no. 2, p. 022703, Feb. 2012.

[116] J. C. Zier, R. M. Gilgenbach, Y. Y. Lau, D. Chalenski, D. M. French, M. R. Gomez, S. G. Patel, I. M. Rittersdorf, A. Steiner, M. Weiss, P. Zhang, M. Mazarakis, M. E. Cuneo, and M. Lopez, "Magneto-Rayleigh-Taylor experiments on a MA linear transformer driver," *Phys. Plasmas*, vol. 19, no. 3, p. 032701, Mar. 2012.

[117] A. R. Miles, "Nonlinear Rayleigh–Taylor instabilities in fast Z pinches," *Phys. Plasmas*, vol. 16, no. 3, p. 032702, Mar. 2009.

[118] D. C. Rovang, D. C. Lamppa, M. E. Cuneo, R. D. McBride, J. McKenney, R. J. Kaye, A. B. Sefkow, and S. A. Slutz, "Magnetic field coil designs for MagLIF," Sandia Nat. Lab., Albuquerque, NM, Tech. Rep. SAND2012-0884C, 2012.

[119] N. B. Meezan, L. Divol, M. M. Marinak, G. D. Kerbel, L. J. Suter, R. M. Stevenson, G. E. Slark, and K. Oades, "Hydrodynamics simu-

lations of 2 ω laser propagation in underdense gasbag plasma," *Phys. Plasmas*, vol. 11, no. 12, pp. 5573–5579, Dec. 2004.

[120] G. B. Zimmerman and W. L. Kruer, "Numerical simulation of laser-initiated fusion," *Comments Plasma Phys. Control. Fusion*, vol. 2, no. 2, pp. 51–61, 1975.

[121] M. M. Marinak, R. E. Tipton, O. L. Landen, T. J. Murphy, P. Amendt, S. W. Haan, S. P. Hatchett, C. J. Keane, R. McEachern, and R. Wallace, "Three-dimensional simulations of Nova high growth factor capsule implosion experiments," *Phys. Plasmas*, vol. 3, no. 5, pp. 2070–2076, May 1996.

[122] D. D. Ryutov, M. E. Cuneo, M. C. Herrmann, D. B. Sinars, and S. A. Slutz, "Simulating the magnetized liner inertial fusion plasma confinement with smaller-scale experiments," *Phys. Plasmas*, vol. 19, no. 6, p. 062706, Jun. 2012.

[123] R. A. Vesey, "Multi-GJ indirect-drive targets for Z-IFE using the double-ended Hohlraum," in *Proc. Z-Inertial Fusion Energy Workshop*, Albuquerque, NM, Aug. 1/2, 2005.

[124] M. G. Mazarakis, W. E. Fowler, K. L. LeChien, F. W. Long, M. K. Matzen, D. H. McDaniel, R. G. McKee, C. L. Olson, J. L. Porter, S. T. Rogowski, K. W. Struve, W. A. Stygar, J. R. Woodworth, A. A. Kim, V. A. Sinebryukhov, R. M. Gilgenbach, M. R. Gomez, D. M. French, Y. Y. Lau, J. C. Zier, D. M. VanDevalde, R. A. Sharpe, and K. Ward, "High-current linear transformer driver development at Sandia National Laboratories," *IEEE Trans. Plasma Sci.*, vol. 38, no. 4, pp. 704–713, Apr. 2010.

[125] M. G. Mazarakis, W. E. Fowler, A. A. Kim, V. A. Sinebryukhov, S. T. Rogowski, R. A. Sharpe, D. H. McDaniel, C. L. Olson, J. L. Porter, K. W. Struve, W. A. Stygar, and J. R. Woodworth, "High current, 0.5-MA, fast, 100-ns, linear transformer driver experiments," *Phys. Rev. ST Accel. Beams*, vol. 12, no. 5, p. 050401, May 2009.

[126] A. A. Kim, M. G. Mazarakis, V. A. Sinebryukhov, B. M. Kovalchuk, V. A. Visir, S. N. Volkov, F. Bayol, A. N. Bastrikov, V. G. Durakov, S. V. Frolov, V. M. Alexeenko, D. H. McDaniel, W. E. Fowler, K. LeChien, C. Olson, W. A. Stygar, K. W. Struve, J. Porter, and R. M. Gilgenbach, "Development and tests of fast 1-MA linear transformer driver stages," *Phys. Rev. ST Accel. Beams*, vol. 12, no. 5, p. 050402, May 2009.

[127] J. R. Woodworth, W. E. Fowler, B. S. Stoltzfus, W. A. Stygar, M. E. Sceiford, M. G. Mazarakis, H. D. Anderson, M. J. Harden, J. R. Blickem, R. White, and A. A. Kim, "Compact 810 kA linear transformer driver cavity," *Phys. Rev. ST Accel. Beams*, vol. 14, no. 4, p. 040401, Apr. 2011.

[128] W. A. Stygar, W. E. Fowler, K. R. LeChien, F. W. Long, M. G. Mazarakis, G. R. McKee, J. L. McKenney, J. L. Porter, M. E. Savage, B. S. Stoltzfus, D. M. Van De Valde, and J. R. Woodworth, "Shaping the output pulse of a linear-transformer-driver module," *Phys. Rev. ST Accel. Beams*, vol. 12, no. 3, p. 030402, Mar. 2009.

[129] W. A. Stygar, private communication, 2011.

[130] C. L. Olson, M. G. Mazarakis, E. Fowler, R. A. Sharpe, D. L. Smith, M. C. Turgeon, W. L. Langston, T. D. Pointon, P. F. Ottinger, J. W. Schumer, D. R. Welch, D. V. Rose, T. C. Genoni, N. L. Bruner, C. Thoma, M. E. Barkey, M. Guthrie, D. C. Kammer, G. L. Kulcinski, Y. G. Kalinin, A. S. Kingsep, S. L. Nedoseev, V. P. Smirnov, and A. Kim, "Recyclable transmission line (RTL) and linear transformer driver (LTD) development for z-pinch inertial fusion energy (Z-IFE) and high yield," Sandia Nat. Lab., Albuquerque, NM, Tech. Rep. SAND2007-0059, 2007.

[131] C. L. Olson, G. Rochau, S. Slutz, C. Morrow, R. Olson, M. Cuneo, D. Hanson, G. Bennett, T. Sanford, J. Bailey, W. Stygar, R. Vesey, T. Mehlhorn, K. Struve, M. Mazarakis, M. Savage, T. Pointon, M. Kiefer, S. Rosenthal, K. Cochrane, L. Schneider, S. Glover, K. Reed, D. Schroen, C. Farnum, M. Modesto, D. Oscar, L. Chhabildas, J. Boyes, V. Vigil, R. Keith, M. Turgeon, B. Cipiti, E. Lindgren, V. Dandini, H. Tran, D. Smith, D. McDaniel, J. Quintenz, M. K. Matzen, J. P. VanDevender, W. Gauster, L. Shephard, M. Walck, T. Renk, T. Tanaka, M. Ulrickson, W. Meier, J. Latkowski, R. Moir, R. Schmitt, S. Reyes, R. Abbott, R. Peterson, G. Pollock, P. Ottinger, J. Schumer, P. Peterson, D. Kammer, G. Kulcinski, L. El-Guebaly, G. Moses, I. Sviatoslavsky, M. Sawan, M. Anderson, R. Bonazza, J. Oakley, P. Meekunasombat, J. De Groot, N. Jensen, M. Abdou, A. Ying, P. Calderoni, N. Morey, S. Abdel-Khalik, C. Dillon, C. Lascar, D. Sadowski, R. Curry, K. McDonald, M. Barkey, W. Szaroletta, R. Gallix, N. Alexander, W. Rickman, C. Charman, H. Shatoff, D. Welch, D. Rose, P. Panchuk, D. Louie, S. Dean, A. Kim, S. Nedoseev, E. Grabovsky, A. Kingsep, and V. Smirnov, "Development path for Z-Pinch IFE," *Fusion. Sci. Technol.*, vol. 47, no. 3, pp. 633–640, Apr. 2005.

[132] K. R. LeChien, W. A. Stygar, M. E. Savage, P. E. Wakeland, V. Anaya, D. S. Artery, M. J. Baremore, D. E. Bliss, R. Chavez, G. D. Coombs, J. P. Corley, P. A. Jones, A. K. Kipp, B. A. Lewis, J. A. Lott, J. J. Lynch, G. R. McKee, S. D. Ploor, K. R. Prestwich, S. A. Roznowski, D. C. Spencer, S. D. White, and J. R. Woodworth, "6.1-MV, 0.79-MA laser-triggered gas switch for multimodule, multiterawatt pulsed-power accelerators," *Phys. Rev. ST Accel. Beams*, vol. 13, no. 3, p. 030401, Mar. 2010.

[133] W. A. Stygar, private communication, 2011.

[134] M. E. Cuneo, M. Herrmann, S. A. Slutz, W. A. Stygar, M. G. Mazarakis, M. E. Savage, W. E. Fowler, D. B. Sinars, R. D. McBride, C. A. Jennings, A. B. Sefkow, R. A. Vesey, C. Nakhleh, J. P. VanDevender, E. M. Waisman, R. G. McKee, A. Owen, D. C. Rovang, J. McKenney, D. C. Lamppa, R. J. Kaye, R. W. Lemke, M. R. Martin, D. G. Flicker, D. L. Hanson, A. J. Lopez, K. P. Shelton, J. M. Villalva, J. L. Porter, M. K. Matzen, and C. L. Olson, "Pulsed power science and technology for inertial fusion energy at Sandia National Laboratories," in *Proc. 24th Symp. Fusion Eng.*, Chicago, IL, Jun. 26-30, 2011.

[135] S. C. Hsu, T. J. Awe, S. Brockington, A. Case, J. T. Cassibry, G. Kagan, S. J. Messer, M. Stanic, X. Tang, D. R. Welch, and F. D. Witherspoon, "Spherically imploding plasma liners as a standoff driver for magnetoinertial fusion," *IEEE Trans. Plasmas Sci.*, vol. 40, no. 5, pp. 1287–1298, May 2012.

[136] D. D. Ryutov, M. S. Derzon, and M. K. Matzen, "The physics of fast Z-pinches," *Rev. Mod. Phys.*, vol. 72, no. 1, p. 167, Jan. 2000.

Authors' photographs and biographies not available at the time of publication.